

The comment by **reviewer #1** is reproduced in a black font below. Our response follows the comment in a blue font. Text additions to the manuscript, for example, significantly modified sentences, appear in the revised manuscript in red color.

The section on limitations has answered some of my reservations. But I would still like to know what the variability is between the three samples at each location as this will improve the comparison between locations. This was not answered in the response.

We thank the reviewer for pointing out this variability between the three samples at each location. The main purpose of this study was to compare the chemical composition of organic compounds in the PM_{2.5} samples collected in the three Chinese cities. Therefore, to reduce the uncertainty caused by the variability between the three samples of each city, only organic compounds measured in all three samples of each city are used for intercity comparison. We have now added the statement in the revised manuscript (Page 7, Line 205-207) as follows:

‘To reduce the uncertainty caused by the variability between the samples collected at each location, only organic compounds measured in all three samples of each city are used for intercity comparison in this study.’

1 **Urban organic aerosol composition in Eastern China differs from North to South: Molecular**
2 **insight from a liquid chromatography-Orbitrap mass spectrometry study**

3 Kai Wang^{1,2,4}, Ru-Jin Huang¹, Martin Brüggemann³, Yun Zhang², Lu Yang¹, Haiyan Ni¹, Jie Guo¹,
4 Meng Wang¹, Jiajun Han⁵, Merete Bilde⁴, Marianne Glasius⁴, and Thorsten Hoffmann²

5 ¹State Key Laboratory of Loess and Quaternary Geology (SKLLQG), Center for Excellence in
6 Quaternary Science and Global Change, and Key Laboratory of Aerosol Chemistry and Physics,
7 Institute of Earth and Environment, Chinese Academy of Sciences, Xi'an 710061, China

8 ²Institute of Inorganic and Analytical Chemistry, Johannes Gutenberg University Mainz,
9 Duesbergweg 10–14, Mainz 55128, Germany

10 ³Atmospheric Chemistry Department (ACD), Leibniz Institute for Tropospheric Research
11 (TROPOS), Permoserstraße 15, 04318 Leipzig, Germany

12 ⁴Department of Chemistry, Aarhus University, Langelandsgade 140, DK-8000 Aarhus C, Denmark

13 ⁵Department of Chemistry, University of Toronto, 80 St. George Street, M5S3H6 Toronto, Canada

14 Corresponding Author: Ru-Jin Huang (rujin.huang@ieecas.cn) and Thorsten Hoffmann
15 (t.hoffmann@uni-mainz.de)

16

17

18

19

20

21

22

23

24

25

26

27 **Abstract:**

28 Air pollution by particulate matter in China affects human health, the ecosystem and the climate.
29 However, the chemical composition of particulate aerosol, especially of the organic fraction, is still
30 not well understood. In this study, particulate aerosol samples with a diameter of $\leq 2.5 \mu\text{m}$ ($\text{PM}_{2.5}$)
31 were collected in January 2014 in three cities located in Northeast, East and Southeast China,
32 namely Changchun, Shanghai and Guangzhou. Organic aerosol (OA) in the $\text{PM}_{2.5}$ samples was
33 analyzed by ultrahigh performance liquid chromatography (UHPLC) coupled to high-resolution
34 Orbitrap mass spectrometry in both negative mode (ESI⁻) and positive mode electrospray
35 ionization (ESI⁺). After non-target screening including the assignment of molecular formulas, the
36 compounds were classified into five groups based on their elemental composition, i.e., CHO,
37 CHON, CHN, CHOS and CHONS. The CHO, CHON and CHN groups present the dominant signal
38 abundances of 81–99.7% in the mass spectra and the majority of these compounds were assigned
39 to mono- and polyaromatics, suggesting that anthropogenic emissions are a major source of urban
40 OA in all three cities. However, the chemical characteristics of these compounds varied between
41 the different cities. The degree of aromaticity and the number of polyaromatic compounds were
42 substantially higher in samples from Changchun, which could be attributed to the large emissions
43 from residential heating (i.e. coal combustion) during winter time in Northeast China. Moreover,
44 the ESI⁻ analysis showed higher H/C and O/C ratios for organic compounds in Shanghai and
45 Guangzhou compared to samples from Changchun, indicating that OA undergoes more intense
46 photochemical oxidation processes in lower latitude regions of China and/or is affected to a larger
47 degree by biogenic sources. The majority of sulfur-containing compounds (CHOS and CHONS) in
48 all cities were assigned to aliphatic compounds with low degrees of unsaturation and aromaticity.
49 Here again, samples from Shanghai and Guangzhou show a greater chemical similarity but differ
50 largely from those from Changchun. It should be noted that the conclusions drawn in this study are
51 mainly based on comparison of molecular formulas weighted by peak abundance, and thus, are
52 associated with inherent uncertainties due to different ionization efficiencies for different organic
53 species.

54 **1. Introduction**

55 In the last decades, China has experienced rapid industrialization and urbanization accompanied by
56 severe and persistent particulate air pollution (Huang et al., 2014; Sun et al., 2014; Ding et al., 2016;
57 Song et al., 2018; Shi et al., 2019; Xu et al., 2019). These particulate air pollution extremes can not
58 only influence the regional air quality and human health in China, but also lead to a global

59 environmental problem due to long-distance transport of pollutants. To better understand the effects
60 of air pollution on air quality and human health, chemical characterization of fine particle
61 (particulate matter with an aerodynamic diameter of less than 2.5 μm , or $\text{PM}_{2.5}$) is crucial. However,
62 the chemical composition of $\text{PM}_{2.5}$ in China is still poorly understood due to a wide variety of
63 natural and anthropogenic sources as well as complex multiphase chemical reactions (Lin et al.,
64 2012a; Huang et al., 2014; Ding et al., 2016; Wang et al., 2017; Wang et al., 2018; An et al., 2019;
65 Tong et al., 2019; Wang et al., 2019a; Wang et al., 2019b). In particular, compared to the fairly
66 well understood nature of the inorganic fraction of aerosol, the organic fraction, also named organic
67 aerosol (OA), is considerably less understood in terms of chemical composition, corresponding
68 precursors, sources and formation mechanisms (Huang et al., 2017).

69 During pollution events in China, OA accounts for as high as more than 50% of the total mass of
70 fine particle (An et al., 2019). Chemical compounds in OA cover a large complexity of species
71 including alcohols, aldehydes, carboxylic acids, imidazoles, organosulfates, organonitrates and
72 polycyclic aromatic hydrocarbons (PAHs) (Lin et al., 2012a; Rincón et al., 2012; Kourtchev et al.,
73 2014; Wang et al., 2018; Elzein et al., 2019; Wang et al., 2019a). Thus, the capacity of traditional
74 analytical techniques is limited to identify the compounds in OA and the majority (> 70%) of OA
75 has not been identified yet as specific compounds (Hoffmann et al., 2011). The insufficient
76 knowledge of chemical composition of OA hinders a better understanding of the sources, formation
77 and atmospheric processes of air pollution in China.

78 Recently, ultrahigh resolution mass spectrometry (UHRMS), such as Fourier transform ion
79 cyclotron resonance mass spectrometry (FTICR-MS) and Orbitrap-MS, coupled with soft
80 ionization sources (e.g., electrospray ionization (ESI) and atmospheric pressure chemical ionization
81 (APCI)) have been introduced to elucidate the molecular composition of OA (Nizkorodov et al.,
82 2011; Lin et al., 2012a; Lin et al., 2012b; Rincón et al., 2012; Noziere et al., 2015; Kourtchev et al.,
83 2016; Tong et al., 2016; Tu et al., 2016; Brüggemann et al., 2017; Wang et al., 2017; Fleming et
84 al., 2018; Laskin et al., 2018; Song et al., 2018; Wang et al., 2018; Brüggemann et al., 2019;
85 Daellenbach et al., 2019; Ning et al., 2019; Wang et al., 2019a). Due to the two outstanding features
86 of high resolving power and high mass accuracy, UHRMS can give precise elemental compositions
87 of individual organic compounds. However, UHRMS studies on Chinese urban OA are very limited.
88 Wang et al. (Wang et al., 2017) characterized OA in Shanghai and showed variations in chemical
89 composition among different months and between daytime and nighttime. Our recent Orbitrap MS
90 study (Wang et al., 2018) showed that wintertime OA in $\text{PM}_{2.5}$ collected in Beijing, China and
91 Mainz, Germany were very different in terms of chemical composition. In contrast, for summertime

92 OA from Germany and China, Brüggemann et al. (2019) found similar compounds and
93 concentrations of terpenoid organosulfates in PM₁₀, demonstrating that biogenic emission can
94 significantly affect OA composition at both locations. Ning et al. (2019) analyzed the OA collected
95 in a coastal Chinese city (Dalian) and found that more organic compounds were identified in haze
96 days compared to non-haze days. Nonetheless, since severe particulate pollution in China occurs
97 on a large-scale, more UHRMS studies are needed to fully elucidate the chemical composition of
98 OA in different Chinese cities.

99 In this study, PM_{2.5} aerosol samples were collected in three Chinese cities, i.e., Changchun,
100 Shanghai and Guangzhou, and their organic fraction was analyzed using ultra-high-performance
101 liquid chromatography (UHPLC) coupled with Orbitrap-MS. The Chinese cities of Changchun,
102 Shanghai and Guangzhou are located in the Northeast, East and Southeast of China, which are
103 major populated regions in China with a population of 7.5, 24 and 15 million, respectively. The
104 geographic locations of these three cities cover a large latitude spanning from 23.12°N to 43.53°N
105 resulting in different meteorological conditions, including intensity and duration of sunlight,
106 average daily temperature and monsoon climate. In addition, the industrial structure, energy
107 consumption and energy sources in these three cities are different, such as much more heavy
108 industries (e.g., coal chemical industry and steelworks) in Northeast China (Zhang, 2008), which
109 can cause difference in anthropogenic emissions, and can therefore influence the chemical
110 composition of urban OA. Moreover, OA is strongly affected by residential coal combustion during
111 winter in Northeast China (Huang et al., 2014; An et al., 2019). Therefore, this study presents a
112 comprehensive overview of chemical composition of OA in three representative Chinese cities
113 during pollution episodes, which eventually can improve our understanding of OA effects on
114 climate and public health and also provide a chemical database for haze mitigation strategies in
115 China.

116 **2. Experimental**

117 **2.1 PM_{2.5} samples**

118 Three 24-h integrated urban PM_{2.5} samples were collected during severe haze pollution events with
119 daily average PM_{2.5} mass concentration higher than 115 µg m⁻³ in each of the three Chinese cities:
120 Changchun (43.54° N, 125.13° E, 1.5 m above the ground), Shanghai (31.30° N, 121.50° E, 20 m
121 above the ground) and Guangzhou (23.07° N, 113.21° E, 53 m above the ground), which are located
122 in the Northeast, East and Southeast regions of China, respectively (see Fig. 1). Samples in
123 Changchun were collected on 4, 24 and 29 of January 2014 with PM_{2.5} mass concentrations of

124 185–222 $\mu\text{g m}^{-3}$, samples in Shanghai were collected on 1, 19 and 20 of January 2014 with $\text{PM}_{2.5}$
125 mass concentrations of 159–172 $\mu\text{g m}^{-3}$ and samples in Guangzhou were collected on 5, 6 and 11
126 of January 2014 with $\text{PM}_{2.5}$ mass concentrations of 138–152 $\mu\text{g m}^{-3}$. Further details (e.g., the daily
127 average concentrations of $\text{PM}_{2.5}$, SO_2 , NO_2 , CO and O_3 , the average temperature and the daily solar
128 radiation value during sampling dates) are presented in Table S1, the 48 hours back trajectories of
129 air arriving at the three sampling sites during the sampling periods are shown in Fig. S1. All $\text{PM}_{2.5}$
130 samples were collected on prebaked quartz-fiber filters (20.3×25.4 cm) using a high-volume $\text{PM}_{2.5}$
131 sampler at a flow rate of 1.05 $\text{m}^3 \text{min}^{-1}$ (Tisch Environmental, USA) and at each sampling site field
132 blanks were taken. After sample collection, filters were stored at $-20\text{ }^\circ\text{C}$ until analysis.

133 **2.2 Sample analysis**

134 Detailed description on the filter sample extraction and UHPLC–Orbitrap MS analysis can be found
135 in our previous studies (Wang et al., 2018; Wang et al., 2019a). Briefly, a part of the filters (around
136 1.13 cm^2 , corresponding to about 600 μg particle mass in each extracted filter) was extracted three
137 times with 1.0–1.5 mL of acetonitrile-water (8/2, v/v) in an ultrasonic bath. The extracts were
138 combined, filtered through a 0.2 μm Teflon syringe filter and evaporated to almost dryness under
139 a gentle nitrogen stream. Finally, the residue was redissolved in 1000 μL acetonitrile-water (1/9,
140 v/v) to reach the total particulate mass concentration of around 600 $\mu\text{g mL}^{-1}$ for the following
141 analysis.

142 Compared to the direct infusion method applied in other UHRMS studies (Lin et al., 2012a; Lin et
143 al., 2012b; Rincón et al., 2012; Kourtchev et al., 2016; Fleming et al., 2018), the UHPLC technique
144 was used in this study, which could separate and concentrate the compounds before they entered
145 the ion source, reducing the ionization suppression and increasing the sensitive of the measurement.
146 In addition, it can provide separation of some compounds and information of retention time of the
147 compounds, which is useful for the identification of the compounds and the separation of isomers.
148 The analytes were separated using a Hypersil Gold column (C18, 50 x 2.0 mm, 1.9 μm particle size)
149 with mobile phases consisting of (A) 0.04% formic acid and 2% acetonitrile in MilliQ water and
150 (B) 2% water in acetonitrile. Gradient elution was applied with the A and B mixture at a flow rate
151 of 500 $\mu\text{L min}^{-1}$ as follows: 0–1.5 min 2% B, 1.5–2.5 min from 2% to 20% B (linear), 2.5–5.5 min
152 20% B, 5.5–6.5 min from 20% to 30% B (linear), 6.5–7.5 min from 30% to 50% B (linear), 7.5–8.5
153 min from 50% to 98% B (linear), 8.5–11.0 min 98% B, 11.0–11.05 min from 98% to 2% B (linear),
154 and 11.05–11.1 min 2% B. The Q Exactive Hybrid Quadrupole-Orbitrap MS was equipped with a
155 heated ESI source at 120 $^\circ\text{C}$, applying a spray voltage of -3.3 kV and 4.0 kV for negative ESI mode

156 (ESI⁻) and positive ESI mode (ESI⁺), respectively. The mass scanning range was set from m/z 50
157 to 500 with a resolving power of 70,000 @ m/z 200. The Orbitrap MS was externally calibrated
158 before each measurement sequence using an Ultramark 1621 solution (Sigma–Aldrich, Germany)
159 providing mass accuracy of the instrument lower than 3 ppm. Each sample was measured in
160 triplicate with an injection volume of 10 µL.

161 **2.3 Data processing**

162 A non-target peak picking software (SIEVE[®], Thermo Fisher Scientific, Germany) was used to find
163 significant peaks in the LC-MS dataset and to calculate all mathematically possible chemical
164 formulas for ions signals with a sample-to-blank abundance ratio ≥ 10 using a mass tolerance of \pm
165 2 ppm. The permitted maximum elemental number of atoms was set as follows: ¹²C (39), ¹H (72),
166 ¹⁶O (20), ¹⁴N (7), ³²S (4), ³⁵Cl (2) and ²³Na (1) (Kind and Fiehn, 2007; Lin et al., 2012a; Wang et
167 al., 2018). To remove the chemically unreasonable formulas, further constraint was applied by
168 setting H/C, O/C, N/C, S/C and Cl/C ratios in the ranges of 0.3–3, 0–3, 0–1.3, 0–0.8 and 0–0.8
169 (Kind and Fiehn, 2007; Lin et al., 2012a; Rincón et al., 2012; Wang et al., 2018; Zielinski et al.,
170 2018), respectively. For chemical formula C_cH_hO_oN_nS_sCl_x, the double bond equivalent (DBE) was
171 calculated by the equation: $DBE = (2c + 2 - h - x + n) / 2$. The aromaticity equivalent (X_C) as a
172 modified index for aromatic compounds was obtained using the equation: $X_C = [3(DBE - (p \times o +$
173 $q \times n)) - 2] / [DBE - (p \times o + q \times n)]$, where p and q, respectively, refer to the fraction of oxygen
174 and sulfur atoms involved in the π -bond structure of a compound. As such the values of p and q
175 vary between compound categories (Yassine et al., 2014). For example, carboxylic acids and esters
176 are characterized using p = q = 0.5, while p = q = 1 and p = q = 0 are used for carbonyl and hydroxyl,
177 respectively. Since it is impossible to identify the structures of the hundreds of formulas observed
178 in this study, we cannot know the exact values of p and q in an individual compound. Therefore, in
179 this study, p = q = 0.5 was applied for compounds detected in ESI⁻ as carboxylic compounds are
180 preferably ionized in negative mode. However, because of the high complexity of the mass spectra
181 in ESI⁺, p = q = 1 was used in ESI⁺ to avoid an overestimation of the amount of aromatics.
182 Moreover, for $DBE \leq (p \times o + q \times n)$ or $X_C \leq 0$, X_C was defined as zero. Furthermore, in ESI⁻, for
183 odd numbers of (p × o + q × n), the value of (p × o + q × n) was rounded down to the lower integer.
184 $X_C \geq 2.50$ and $X_C \geq 2.71$ have been suggested as unambiguous minimum criteria for the presence
185 of monoaromatics and polyaromatics, respectively (Yassine et al., 2014).

186 Comparing the peak abundance has been used in recent UHRMS studies (Wang et al., 2017;
187 Fleming et al., 2018; Song et al., 2018; Ning et al., 2019) to illustrate the relative importance of

188 specific types of compounds. However, it should be noted that different organic compounds have
189 different signal response in the mass spectrometer due to the differences in ionization and
190 transmission efficiencies (Schmidt et al., 2006; Leito et al., 2008; Perry et al., 2008; Krueve et al.,
191 2014). Therefore, uncertainties may exist when comparing the peak areas among compounds. In
192 this work, we assume that all organic compounds have the same peak abundance response in the
193 mass spectrometer. The peak abundance-weighted average molecular mass (MM), elemental ratios,
194 DBE, and Xc for formula $C_cH_hO_oN_nS_sCl_x$ were calculated using following equations:

$$195 \quad MM_{avg} = \sum (MM_i \times A_i) / \sum A_i$$

$$196 \quad O/C_{avg} = \sum (O/C_i \times A_i) / \sum A_i$$

$$197 \quad H/C_{avg} = \sum (H/C_i \times A_i) / \sum A_i$$

$$198 \quad DBE_{avg} = \sum (DBE_i \times A_i) / \sum A_i$$

$$199 \quad Xc_{avg} = \sum (Xc_i \times A_i) / \sum A_i$$

200 where A_i is the peak abundance for each individual compound i .

201 **3. Results and discussion**

202 **3.1 General characteristics**

203 The main purpose of this study was to tentatively identify and compare the chemical composition
204 of organic compounds in the $PM_{2.5}$ samples collected in the three Chinese cities: Changchun,
205 Shanghai and Guangzhou during pollution episodes. [To reduce the uncertainty caused by the](#)
206 [variability between the samples collected at each location, only organic compounds measured in](#)
207 [all three samples of each city are used for intercity comparison in this study.](#) The number of organic
208 compounds and molecular formulas detected in each city, the peak abundance-weighted average
209 values of molecular mass (MM_{avg}), elemental ratios, DBE, Xc and the isomer number fraction
210 (meaning the percentage of formula numbers that have isomers among all assigned formulas) for
211 each subgroup are listed in Table 1. It should be noted that in this study we focus solely on organic
212 compounds with elevated signal abundances, and thus, presumably rather high concentrations. In
213 contrast to our previous study (Wang et al., 2018), compounds with low concentrations were
214 excluded by increasing the reconstitution volume from 500 μ L to 1000 μ L, reducing the sample
215 injection volume from 20 μ L to 10 μ L, and increasing the sample-to-blank ratio from 3 to 10 during
216 data processing.

217 Overall, 416–769 (assigned to 272–415 molecular formulas) and 687–2943 (assigned to 383–679
218 molecular formulas) organic compounds in different samples were determined in ESI⁻ and ESI⁺,
219 respectively. The largest number of organic compounds was observed in Changchun samples in
220 both ESI⁻ and ESI⁺, indicating that OA collected during winter season in Northeast China was
221 more complex compared to urban OA in East and Southeast China. This increased number of
222 compounds can possibly be explained by the large residential coal combustion emissions in winter
223 in North China (Huang et al., 2014; Song et al., 2018; An et al., 2019). In addition, ambient
224 temperatures were lowest during the sampling period in Changchun (i.e., -14 °C to -9 °C, Table
225 S1), which likely led to a decreased boundary layer height and therefore enhanced accumulation of
226 pollutants and enhanced formation of secondary organic aerosol through for example gas-to-
227 particle partitioning.

228 As shown in Table 1, the abundance-weighted average values of MM_{avg} and O/C ratio of the total
229 assigned formulas for Changchun samples detected in negative mode (Changchun⁻) are 169 and
230 0.58, respectively, which are lower than those for Shanghai⁻ ($MM_{avg} = 176$ and $O/C = 0.69$) and
231 for Guangzhou⁻ ($MM_{avg} = 183$ and $O/C = 0.74$). On the contrary, the aromaticity equivalent X_c for
232 organics detected in Changchun⁻, $X_c(\text{Changchun}^-) = 2.13$, is substantially higher than that for
233 Shanghai⁻, $X_c(\text{Shanghai}^-) = 1.92$, and Guangzhou⁻, $X_c(\text{Guangzhou}^-) = 1.65$. These observations
234 indicate that urban OA in Northeast China features a lower degree of oxidation and a higher degree
235 of aromaticity compared to urban OA in East and Southeast China. Furthermore, the relative peak
236 abundance fraction of compounds with $O/C \geq 0.6$, which are considered as highly oxidized
237 compounds (Tu et al., 2016), is 31% in Changchun⁻, and higher in Shanghai⁻ (46%) and
238 Guangzhou⁻ (51%). The different chemical composition of the samples is probably caused by the
239 rather low ambient temperatures and decreased photochemical processing of organic compounds
240 in Northeast China (indicated by the lower solar radiation in Northeast China, see Table S1),
241 slowing down oxidation processes and leading to a larger number of PAHs, which are mainly
242 emitted from coal burning (Huang et al., 2014; Song et al., 2018) or by different
243 biogenic/anthropogenic precursors. In addition, long-range transport of air masses (see the 48 hours
244 back trajectories in Fig. S1) may have a certain effect on the chemical properties of aerosol samples
245 collected in the three cities.

246 Figure 1 shows the reconstructed mass spectra of organic compounds detected in ESI⁻ and ESI⁺.
247 A major fraction organic species detected in ESI⁻ are attributed to CHO⁻ and CHON⁻, accounting
248 for 30–42% and 39–55% in terms of peak abundance, respectively, and comprising 39–45% and
249 23–33% in terms of peak numbers, respectively. This is consistent with previous studies on Chinese

250 urban OA by Wang et al. (2017 and 2018) and Brüggemann et al. (2019). Comparing the organic
251 compounds detected in ESI⁻ for the three cities, 120 formulas were observed in all cities as
252 common formulas (which refer to the compounds detected in all cities with the same molecular
253 formulas and with the same retention times (retention time difference ≤ 0.1 min)) (Fig. 2a),
254 accounting for 29–44% and 57–71% of all assigned formulas in terms of formula numbers and
255 peak abundance, respectively. Despite the above-mentioned differences in chemical composition
256 for OA from Changchun compared to OA from Shanghai and Guangzhou, these results demonstrate
257 that still a large number of common organic compounds exist in Chinese urban OAs collected in
258 different cities, in particular for organics with higher signal abundances. Furthermore, as shown by
259 the pie chart in Fig. 2b, these common formulas are dominated by CHON⁻ and CHO⁻, accounting
260 for 62% and 30% of the total common formulas in terms of peak abundance, respectively.

261 As it is commonly known, ESI exhibits different ionization mechanisms in negative and positive
262 ionization modes. While ESI⁻ is especially sensitive to deprotonatable compounds (e.g., organic
263 acids), ESI⁺ is more sensitive to protonatable compounds (e.g., organic amines) (Ho et al., 2003).
264 Due to the different ionization mechanisms, clear differences were observed in the mass spectra
265 (Fig. 1) and chemical characteristics (Table 1) from ESI⁻ and ESI⁺ measurements. For example,
266 CHO compounds were preferentially detected in ESI⁻, accounting for a relatively large fraction of
267 30–42% of all detected compounds in terms of peak abundance, compared to merely 4–13% for
268 such CHO compounds in ESI⁺. In contrast, CHN compounds were only observed in ESI⁺, yielding
269 a rather large peak abundance fraction of 40–71%. In particular, as can be seen in Fig.1, several
270 peaks of CHN⁺ compounds in Shanghai⁺ and Guangzhou⁺ have much higher abundance compared
271 to other organic species, probably due to their high concentrations and/or high ionization
272 efficiencies in the positive mode. This observation indicates that most CHO compounds with high
273 concentrations are probably organic acids, whereas the majority of CHN compounds likely belong
274 to the group of organic amines, which is in good agreement with previous studies (Lin et al., 2012a;
275 Wang et al., 2017; Wang et al., 2018). Organic compounds in ESI⁺ are dominated by CHN⁺ and
276 CHON⁺ compounds in terms of both peak numbers and peak abundance and these compounds are
277 characterized by rather high H/C ratio and low O/C ratios (Table 1), indicating a low degree of
278 oxidation. The Venn diagram presented for ESI⁺ measurements in Fig. 2a shows that out of a total
279 of 383–679 formulas, 129 formulas were found in samples from all three cities. Such common
280 formulas, thus, account for 19–34% and 30–75% of all assigned formulas in terms of formula
281 numbers and peak abundance, respectively. Among these common formulas, CHN⁺ and CHON⁺
282 exhibit the highest abundance fractions of 72% and 26%, respectively (Fig. 2b).

283 In the following, we will compare and discuss the chemical properties in detail for the three cities,
284 including degrees of oxidation, unsaturation and aromaticity of each organic compound class (i.e.,
285 CHO, CHON, CHN, CHOS and CHONS). It should be noted that the chlorine-containing
286 compounds were not discussed in this study due to the very low MS signal abundance. In addition,
287 since peak abundances for the formula can vary by orders of magnitude, the area of the circles
288 presented in the Figure 3 and Figures 5–7 is proportional to the fourth root of the peak abundance
289 of each formula to reduce the size difference of the circles. For a more detailed comparison, figures
290 with the circle size related to the absolute peak abundances are presented in the SI.

291 **3.2 CHO compounds**

292 CHO compounds have been widely observed in urban OA, accounting for a substantial fraction
293 (8–67%) of OA (Rincón et al., 2012; Tao et al., 2014; Wang et al., 2017; Wang et al., 2018).
294 Previous studies have shown that a large fraction of CHO compounds in urban OA is composed of
295 organic acids, containing deprotonatable carboxyl functional groups, which are detected
296 preferentially in negative ionization mode when using ESI–MS. As shown in Table 1, a total of
297 346, 164, and 196 CHO– compounds were detected in ESI– in the OA samples collected in
298 Changchun, Shanghai and Guangzhou, accounting for 30%, 40% and 42% of the overall peak
299 abundance in each sample, respectively. Out of all assigned formulas, 47 common CHO– formulas
300 were observed for all cities, accounting for 35–52% and 42–68% of all identified CHO– formulas
301 in terms of formula numbers and peak abundance, respectively.

302 Despite this similarity, OA samples from Changchun– (i.e. in negative ionization mode) exhibit
303 certain differences compared to samples from Shanghai– and Guangzhou–. The average H/C
304 values for CHO– compounds are in a similar range for the three locations (i.e., 0.96–1.10), however,
305 the average O/C values for O/C(Shanghai–) = 0.59 and O/C(Guangzhou–) = 0.65 are rather high
306 compared to the average O/C ratio for Changchun–, O/C(Changchun–) = 0.41. Furthermore, the
307 relative peak abundance fraction of CHO– compounds with O/C ≥ 0.6, which are considered as
308 highly oxidized compounds (Tu et al., 2016), is 14% in Changchun and somewhat higher in
309 Shanghai– (34%) and Guangzhou– (45%). Altogether, these results indicate that CHO– compounds
310 in urban OA from East and Southeast China experienced more intense oxidation and aging
311 processes and/or were affected to a larger degree by biogenic sources.

312 Similarly, as shown in Fig. 3, the abundance-weighted average molecular formulas for CHO–
313 compounds in Changchun–, Shanghai– and Guangzhou– are C_{8.58}H_{7.86}O_{3.22} (MM_{avg}(Changchun–)
314 = 162), C_{8.01}H_{7.27}O_{4.22} (MM_{avg}(Shanghai–) = 171) and C_{7.70}H_{8.04}O_{4.48} (MM_{avg}(Guangzhou–) = 172),

315 respectively. Again, these average formulas show that CHO⁻ in Shanghai⁻ and Guangzhou⁻
316 experienced more intense oxidation processes and/or were affected to a larger degree by biogenic
317 precursors, indicated by the larger abundance-weighted MM_{avg} with a higher degree of oxygenation.
318 In contrast, CHO⁻ compounds from OA samples in Changchun⁻ exhibit a lower abundance-
319 weighted MM_{avg} with a decreased oxygen content.

320 Besides oxygenation, the aromaticity of the detected CHO⁻ compounds exhibits remarkable
321 differences in these three cities. In all cities, the CHO⁻ compounds with high peak abundance were
322 mainly assigned to monoaromatics with $2.5 \leq X_c < 2.7$ (purple circles in Fig. 3) in the region of
323 7–12 carbon atoms per compound and DBE values of 5–7. The relative peak abundance fraction
324 of monoaromatics in total CHO⁻ compounds is 67% in Changchun, which is higher compared to
325 64% in Shanghai and 49% in Guangzhou. In addition, 14% of CHO⁻ compounds in Changchun
326 were identified as polyaromatic compounds with $X_c \geq 2.7$ (red circles in Fig. 3), which is higher
327 than the 8% in Shanghai and 4% in Guangzhou. These observations indicate that CHO⁻ compounds
328 in the three Chinese cities are highly affected by aromatic precursors (e.g., benzene, toluene and
329 naphthalene), in particular for the Changchun aerosol samples.

330 Besides the monoaromatics and polyaromatics, the rest of the detected CHO⁻ compounds were
331 assigned to aliphatic compounds with an X_c lower than 2.5 (grey circles in Fig. 3). Interestingly,
332 these aliphatic compounds account for about 47% of all CHO⁻ compounds for Guangzhou⁻
333 samples in terms of peak abundance, whereas samples from Changchun⁻ and Shanghai⁻ exhibit
334 only rather small fractions of such CHO⁻ compounds, i.e., 19% and 28%, respectively. Such
335 aliphatic compounds are commonly derived from biogenic precursors (Kourtchev et al., 2016) and
336 vehicle emission (Tao et al., 2014; Wang et al., 2017) and/or generated by intense oxidation
337 processes of aromatic precursors, indicating the different biogenic and anthropogenic emission
338 sources and chemical reaction processes for OAs in the three cities.

339 In addition, through the analysis of individual formulas, we find that for the Changchun⁻ samples,
340 formulas of C₈H₆O₄, C₇H₆O₂, C₇H₆O₃, C₈H₈O₂, and C₈H₈O₃ with DBE values of 6, 5, 5, 5, and 5
341 dominate the assigned CHO formulas with respect to peak abundance. According to previous
342 studies, C₈H₆O₄, C₇H₆O₂ and C₇H₆O₃ are suggested to be phthalic acid, benzoic acid and
343 monohydroxy benzoic acid, respectively, which are derived from naphthalene (Kautzman et al.,
344 2010; Riva et al., 2015; Wang et al., 2017; He et al., 2018; Huang et al., 2019). C₈H₈O₂ is likely 4-
345 hydroxy acetophenone, which could be derived from estragole (Pereira et al., 2014), while C₈H₈O₃
346 is suggested to be either 4-methoxybenzoic acid generated from estragole (Pereira et al., 2014) or

347 vanillin emitted from biomass burning (Li et al., 2014). For the Shanghai- samples, besides $C_8H_6O_4$,
348 $C_7H_6O_3$ and $C_7H_6O_2$, formulas of $C_6H_8O_7$ and $C_9H_8O_4$ with DBE values of 3 and 6 were observed
349 with high peak abundances. $C_6H_8O_7$ was identified as citric acid in the pollen sample and mountain
350 particle sample in previous studies (Fu et al., 2008; Wang et al., 2009; Jung and Kawamura, 2011),
351 and $C_9H_8O_4$ are probably homophthalic acid derived from e.g. estragole (Pereira et al., 2014). For
352 the Guangzhou- samples, besides the formulas of $C_8H_6O_4$ and $C_6H_8O_7$ discussed above, $C_4H_6O_4$
353 and $C_4H_6O_5$ with low DBE values of two were detected with high abundances and are suggested to
354 be succinic acid and malic acid, respectively (Claeys et al., 2004; Wang et al., 2017).

355 3.3 CHON compounds

356 A large amount of nitrogen-containing organic compounds was detected in these three cities,
357 accounting for 39–55% and 25–47% of total peak abundance detected in ESI- and ESI+,
358 respectively. Out of all assigned formulas, 45 common CHON- and 62 common CHON+ formulas
359 were observed in all cities, accounting for 65–82% and 25–44% of all CHON compounds detected
360 in ESI- and ESI+ in terms of peak abundance, respectively. It indicates that a large amount of
361 CHON compounds in all three Chinese cities show similar properties of chemical composition.

362 The CHON compounds were further classified into different subgroups according to their O/N
363 ratios (Fig. 4 for CHON- and Fig. S3 for CHON+) or according to the number of nitrogen atoms
364 in their molecular formulas (see Fig. S4 for CHON- and S5 for CHON+). As shown in Fig. 4, the
365 majority (84–96% in terms of peak abundance) of CHON- compounds exhibited O/N ratios ≥ 3 ,
366 allowing the assignment of one nitro ($-NO_2$) or nitrooxy ($-ONO_2$) group for these formulas, which
367 are preferentially ionized in ESI- mode (Lin et al., 2012b; Wang et al., 2017; Song et al., 2018;
368 Wang et al., 2018). CHON- formulas with O/N ratios ≥ 4 suggest the presence of further
369 oxygenated functional groups, such as a hydroxyl group ($-OH$) or a carbonyl group ($C=O$). In
370 terms of peak abundance, 59% of CHON- compounds observed in Guangzhou- exhibited formulas
371 with O/N ratios ≥ 4 , which is higher than 51% in Changchun- and 45% in Shanghai-, indicating
372 that CHON- compounds in Southeast China show a higher degree of oxidation compared to those
373 in Northeast and East China. Not surprisingly, CHON+ compounds generally exhibit lower O/N
374 ratios (Fig. S3), as they probably contain reduced nitrogen functional group (e.g., amines) which
375 are preferably detected in ESI+. As shown in Fig. S3, CHON+ compounds with O/N ratio of 1 are
376 dominant in Changchun+, whereas CHON+ compounds in Shanghai+ and Guangzhou+ show a
377 broader range of O/N ratios from 1 to 3. Moreover, the average O/C ratios (0.27–0.45) in Shanghai+
378 and Guangzhou+ (Table 1) are much greater than that (0.19) in Changchun+. Consistent with the

379 observations for CHO compounds, these results indicate again that CHON⁺ compounds in the OA
380 of East and Southeast China experienced more intensive photooxidation and/or were affected to a
381 larger degree by biogenic precursors.

382 Figure 5 shows the DBE versus C number of CHON⁻ compounds for the three cities. The majority
383 of CHON⁻ compounds lie in the region of 5–15 C atoms and 3–10 DBEs. 67% of CHON⁻
384 compounds in terms of peak abundance were assigned to mono or polyaromatics in Shanghai⁻,
385 which is higher than 52% in Guangzhou⁻ and 55% in Changchun⁻. It indicates that CHON⁻
386 compounds are dominated with aromatic compounds in all cities, while relatively higher peak
387 abundance weighted fraction of aromatic CHON⁻ compounds were observed in Shanghai. The
388 peak abundance-weighted average molecular formulas for CHON⁻ compounds in Changchun⁻,
389 Shanghai⁻ and Guangzhou⁻ are $C_{7.10}H_{6.76}O_{3.56}N_{1.03}$, $C_{7.07}H_{6.03}O_{3.80}N_{1.24}$ and $C_{7.12}H_{6.36}O_{3.99}N_{1.24}$,
390 respectively, showing that CHON⁻ formulas in Shanghai⁻ and Guangzhou⁻ contain more O and
391 N atoms on average than those for Changchun⁻. Formulas of $C_6H_5O_3N_1$, $C_6H_5O_4N_1$, $C_7H_7O_3N_1$,
392 $C_7H_7O_4N_1$, $C_8H_9O_3N_1$, and $C_8H_9O_4N_1$ were detected with the highest abundance in all cities. These
393 molecular formulas are in line with nitrophenol or nitrocatechol analogs, which have been identified
394 in a previous urban OA study (Wang et al., 2017). Furthermore, these nitrooxy-aromatic
395 compounds were shown to enhance light absorbing properties of OA (Laskin et al., 2015; Lin et al.,
396 2015). In addition, it should be noted that the X_c values for $C_6H_5O_4N_1$, $C_7H_7O_4N_1$ and $C_8H_9O_4N_1$
397 were calculated to be lower than 2.5, suggesting that the fraction of aromatics in CHON⁻
398 compounds was underestimated. This is because that for nitrocatechol analogs with formulas of
399 $C_6H_5O_4N_1$, $C_7H_7O_4N_1$ and $C_8H_9O_4N_1$, only one oxygen atom is involved in the π -bond structure
400 corresponding to the p value of 0.25 in the X_c calculation equation, which is lower than the p value
401 of 0.5 applied for the X_c calculation in this study. The diagram of DBE versus C number for
402 CHON⁺ compounds observed in the three locations (presented in Fig. S7 in SI) shows that more
403 aromatic CHON⁺ compounds with relatively lower degree of oxidation were assigned in
404 Changchun⁺ samples compared to Shanghai⁺ and Guangzhou⁺ samples.

405 **3.4 CHN⁺ compounds**

406 696 CHN⁺ compounds were detected in Changchun⁺ samples in ESI⁺, which is higher than in
407 Shanghai⁺ (253) and Guangzhou (205). These CHN⁺ compounds are likely assignable to amines
408 according to previous studies (Rincón et al., 2012; Wang et al., 2017; Wang et al., 2018). The
409 number of CHN⁺ compounds accounts for 24%, 36% and 30% of the total organic compounds in
410 Changchun⁺, Shanghai⁺ and Guangzhou⁺, respectively, whereas the peak abundance of these

411 compounds accounts for 40%, 71% and 62%, respectively. The majority (> 97% in terms of peak
412 abundance) of CHN⁺ compounds have one or two nitrogen atoms in their molecular formulas (see
413 Fig. S9). Comparing the CHN⁺ compounds for the three cities, 51 common CHN⁺ formulas were
414 observed in all cities, which contribute to as much as 43–89% of the total abundance of CHN⁺
415 formulas. This large percentage indicates that CHN⁺ compounds with presumably high
416 concentrations in Changchun⁺, Shanghai⁺ and Guangzhou⁺ exhibit similar chemical composition.
417 However, again OA samples from Changchun show some distinct differences to samples from
418 Guangzhou and Shanghai.

419 A van Krevelen diagram of CHN⁺ compounds detected in the three samples is shown in Fig. 6,
420 illustrating H/C ratios as a function of N/C ratio. In this plot, major parts of the CHN⁺ compounds
421 are found in a region, which is constraint by H/C ratios between 0.5 and 2 and N/C ratios lower
422 than 0.5. Moreover, the pie charts show that the majority (83–87% in terms of peak abundance and
423 72–90% in terms of peak numbers) of these CHN⁺ compounds can be assigned to mono- and
424 polyaromatics with $X_c \geq 2.5$. In addition, as shown in Table 1, the average DBE and X_c values of
425 CHN⁺ compounds are the highest among all organic species. These observations imply that CHN⁺
426 compounds exhibit the highest degree of aromaticity of all organics in the Chinese urban OA
427 samples, which is consistent with previous studies (Lin et al., 2012b; Rincón et al., 2012; Wang et
428 al., 2018). Polyaromatic compounds with $X_c \geq 2.7$ are displayed in the lower left corner of the
429 van Krevelen diagram, accounting for 41% in terms of peak abundance (48% in terms of peak
430 numbers) of CHN⁺ compounds detected in Changchun⁺, but merely for 9–10% in terms of peak
431 abundance (27–31% in terms of peak numbers) in Shanghai⁺ and Guangzhou⁺. For example,
432 formulas of $C_{11}H_{11}N_1$ ($X_c = 2.7$), $C_{10}H_9N_1$ ($X_c = 2.7$), and $C_{12}H_{13}N_1$ ($X_c = 2.7$), which are assigned
433 to be naphthalene core structure-containing compounds, have relatively higher abundance in
434 Changchun⁺ than in Shanghai⁺ and Guangzhou⁺. Moreover, the average DBE and X_c values of
435 CHN⁺ compounds (see Table 1) in Changchun⁺ are substantially higher than those in Shanghai⁺
436 and Guangzhou⁺, further indicating that CHN⁺ compounds in Changchun⁺ show a higher degree
437 of aromaticity, which can be caused by large coal combustion emissions in the winter in Changchun.
438 Remarkably, as can be seen in Fig. 6, the abundance of CHN⁺ compounds in Changchun⁺
439 distributes evenly among different individual CHN⁺ compounds, while in Shanghai⁺ and
440 Guangzhou⁺ they are dominated by the formula of $C_{10}H_{14}N_2$ (the biggest purple circle in Fig. 6)
441 with DBE value of 5, which probably has high concentration and/or high ionization efficiency in
442 the positive ESI mode. According to a previous smog chamber study (Laskin et al., 2010), most
443 CHN⁺ aromatics are probably generated from biomass burning through the addition of reduced

444 nitrogen (e.g., NH₃) to the organic molecules via imine formation reaction, indicating that biomass
445 burning probably made a certain contribution to the formation of CHN⁺ compounds observed in
446 the three urban OA samples in our study.

447 **3.5 CHOS⁻ compounds**

448 In this study, 75–155 CHOS⁻ compounds were observed, accounting for 10%, 12% and 14% of
449 the total peak abundance of all organics in Changchun⁻, Shanghai⁻ and Guangzhou⁻, respectively.
450 Around 89–96% of these CHOS⁻ compounds were found to fulfill the O/S ≥ 4 criterion allowing
451 the assignment of at least one –OSO₃H functional group, and thus, a tentative classification to
452 organosulfates (OSs) (Lin et al., 2012a; Lin et al., 2012b; Tao et al., 2014; Wang et al., 2016; Wang
453 et al., 2017; Wang et al., 2018; Wang et al., 2019a). OSs were shown to affect the surface activity
454 and hygroscopic properties of the aerosol particles, leading to potential impacts on climate (Hansen
455 et al., 2015; Wang et al., 2019a). Out of all formulas, 23 common CHOS⁻ formulas were detected
456 for the three sample locations, accounting for 28%, 58% and 52% of the CHOS⁻ peak abundance
457 in Changchun⁻, Shanghai⁻ and Guangzhou⁻, respectively. However, 40 common CHOS⁻
458 formulas were found between Shanghai⁻ and Guangzhou⁻, accounting for 60–65% and 78–81%
459 in terms of the CHOS⁻ formula numbers and peak abundance, respectively. This indicates that the
460 chemical composition of the major CHOS⁻ compounds of Shanghai⁻ and Guangzhou⁻ are quite
461 similar, while they show substantial chemical differences for samples from Changchun⁻.

462 Figure 7 shows the DBEs as a function of carbon number for all CHOS⁻ compounds detected for
463 the three cities. The CHOS⁻ compounds exhibit a DBE range from 0 to 10 and carbon number
464 range of 2–15. However, the majority of CHOS⁻ compounds with elevated peak abundances
465 concentrate in a region with rather low DBE values of 0–5. The average H/C ratios of CHOS⁻
466 compounds are in the range of 1.56–1.85, and thus, higher than for any other compound class,
467 whereas the average DBE values of 1.71–2.55 are the lowest among all classes. This indicates that
468 CHOS⁻ compounds in the OA from the three Chinese cities are characterized by a low degree of
469 unsaturation. Moreover, the pie charts in Fig. 7 show that aliphatic compounds with X_c ≤ 2.5 are
470 dominant in CHOS⁻ compounds with a fraction of 96–99% in terms of peak abundance, which is
471 substantially higher than that (13–48%) for CHO, CHON and CHN species. Aliphatic CHOS⁻
472 compounds with C ≤ 10 can be formed from biogenic and/or anthropogenic precursors (Hansen
473 et al., 2014; Glasius et al., 2018; Wang et al., 2019a), such as C₂H₄O₆S₁ (derived from glyoxal)
474 (Lim et al., 2010; McNeill et al., 2012), C₃H₆O₆S₁ (derived from isoprene) (Surratt et al., 2007) and
475 C₈H₁₆O₄S₁ (derived from α-pinene). However, more CHOS⁻ compounds with C > 10 and with

476 DBEs lower than 1 are observed in Changchun-, such as $C_{14}H_{28}O_5S_1$, $C_{13}H_{26}O_5S_1$, $C_{12}H_{24}O_5S_1$,
477 $C_{11}H_{22}O_5S_1$ and $C_{11}H_{20}O_6S_1$. These high-carbon-number-containing CHOS- compounds are likely
478 formed from long-alkyl-chain compounds with less oxygenated functional groups, which were
479 previously suggested to be emitted from traffic (Tao et al., 2014) or derived from sesquiterpene
480 emissions (Brüggemann et al., 2019). However, as sesquiterpene emissions can be expected to be
481 very low in wintertime at Changchun, the presence of these compounds further underlines the
482 strong impact of anthropogenic emissions on CHOS- formation in Changchun-. In this study,
483 (O-3S)/C ratio was used instead of traditional O/C ratio to present the oxidation state of CHOS-
484 compounds, since the sulfate functional group contains three more oxygen atoms than common
485 oxygen-containing groups (e.g., hydroxyl and carbonyl), which makes no contribution to the
486 oxidation state of the carbon backbone of the CHOS- compounds. Comparing average values for
487 H/C, (O-3S)/C and DBEs of CHOS- for the three sample locations (see Table 1), we find that the
488 H/C ratios (1.85) and (O-3S)/C ratios (0.61-0.71) for Shanghai- and Guangzhou- samples are
489 larger than those for Changchun- samples (H/C = 1.56 and (O-3S)/C = 0.52), whereas the DBE
490 values (1.71-1.79) in Shanghai- and Guangzhou- are lower than those for Changchun- (2.55).
491 These observations indicate that CHOS- compounds in urban OA from Northeast China are less
492 oxidized but more unsaturated compared to those in East and Southeast China, likely due to
493 enhanced emissions from residential heating during winter in North China.

494 **3.6 CHONS compounds**

495 4-5% of the total organics detected in ESI- were identified as CHONS- compounds in terms of
496 peak abundance. In contrast, CHONS+ compounds account merely for 0.3-1% of all organics
497 detected in ESI+. The average MM_{avg} of the CHONS- compounds for the three sample locations
498 ranges from 214 to 293 Da, generally showing larger molecular masses than compounds of any
499 other class because of the likely presence of both nitrate and sulfate functional groups. In total, only
500 5 common CHONS- formulas were detected for all three sample locations, accounting for 4%, 21%
501 and 20% of the CHONS- peak abundance in Changchun-, Shanghai- and Guangzhou-
502 respectively. As already observed for other compound classes, these percentages imply that the
503 CHONS- compounds in urban OA of Shanghai- and Guangzhou- exhibit a rather similar chemical
504 composition, whereas such compounds are different for Changchun-.

505 In the OA samples of Shanghai- and Guangzhou-, 78-87% of CHONS- compounds in terms of
506 peak abundance have 7 or more O atoms in their formulas, allowing the assignment of one -OSO₃H
507 and one -NO₃ functional groups in the molecular structures, thus, classifying them as potential

508 nitrooxy-organosulfates. In contrast to Shanghai- and Guangzhou-, only 26% of CHONS-
509 compounds were assigned to such nitrooxy-organosulfates for Changchun-, indicating that most
510 of the N atoms in the CHONS- compounds are present in a reduced oxidation state, e.g., in the
511 form of amines. The average DBE and Xc values of CHONS- compounds in Shanghai- and
512 Guangzhou- are 3.3–3.45 and 0.43–0.44, respectively. Again these values differ for the
513 Changchun- samples with an increased average DBE of 3.75 and an average Xc of 1.06, indicating
514 that CHONS- compounds in Changchun- possess on average a higher degree of unsaturation and
515 aromaticity compared to such compounds in Shanghai- and Guangzhou- samples. Interestingly,
516 the compound with formula $C_{10}H_{17}O_7NS$ has the highest relative peak abundance (32%) in
517 Shanghai- and Guangzhou-, whereas in Changchun- the compound with formula $C_2H_3O_4NS$ is
518 dominant. $C_{10}H_{17}O_7NS$ has previously been identified as mononitrate organosulfate generated from
519 α/β -pinene (Iinuma et al., 2007; Surratt et al., 2008; Lin et al., 2012b; Wang et al., 2017), while
520 $C_2H_3O_4NS$ may be assigned as a cyanogroup-containing sulfate. This observation is comparable to
521 our previous study (Wang et al., 2019a), which found that $C_{10}H_{17}O_7NS$ was dominant for CHONS-
522 compounds in low-concentration aerosol samples collected in Beijing (China) and Mainz
523 (Germany). Consistently, a $C_2H_3O_4NS$ compound had the highest abundance among CHONS-
524 compounds in polluted Beijing aerosol samples. This agreement can be explained by the adjacent
525 locations of Beijing (39.99° N, 116.39° E) and Changchun (43.54° N, 125.13° E) and similar
526 residential heating patterns by coal combustion during wintertime. In conclusion, these results
527 further demonstrate that the precursors for CHONS- compounds in Shanghai- and Guangzhou-
528 are different from those in Changchun-, which is probably due to differences in anthropogenic
529 emissions.

530 **4 Conclusion**

531 The molecular composition of the organic fraction of $PM_{2.5}$ samples collected in three Chinese
532 megacities (Changchun, Shanghai and Guangzhou) was investigated using a UHPLC-Orbitrap
533 mass spectrometer. In total, 416–769 (ESI-) and 687–2943 (ESI+) organic compounds were
534 observed and separated into five subgroups: CHO, CHN, CHON, CHOS and CHONS. Specifically,
535 120 common formulas were detected in ESI- and 129 common formulas in ESI+ for all sample
536 locations, accounting for 57–71% and 30–75% in terms of peak abundance, respectively. Overall,
537 we found that urban OA in Changchun, Shanghai and Guangzhou shows a quite similar chemical
538 composition for organic compounds of high concentrations. The majority of these organic species
539 was assigned to mono-aromatic or poly-aromatic compounds, indicating that anthropogenic
540 emissions are the major source for urban OA in all three cities.

541 Despite the chemical similarity of the three sample locations for organic compounds in urban OA,
542 remarkable differences were found in chemical composition of the remaining particle constituents,
543 in particular for OA samples from Changchun. In general, a larger amount of polyaromatics was
544 observed for Changchun samples, most likely due to emissions from coal combustion during
545 wintertime residential heating period. Moreover, the peak abundance-weighted average DBE and
546 average Xc values of the total organic compounds in Changchun were found to be larger than those
547 for Shanghai and Guangzhou, showing that organic compounds in Changchun possess a higher
548 degree of unsaturation and aromaticity. For average H/C and O/C ratios a similar trend was
549 observed. While average H/C and O/C ratios detected in ESI⁻ were found to be highest for
550 Guangzhou samples, relatively lower values were observed for Shanghai and Changchun samples,
551 indicating that OA collected in lower latitude regions of China experiences more intense
552 photochemical oxidation processes and/or are affected to a larger degree by biogenic sources.

553 **5 Limitations**

554 In this study, we used the peak abundance-weighted method to illustrate the difference in chemical
555 formulas assigned by Orbitrap mass spectrometry. This comparison was made based on the
556 assumption that the measured organic compounds have same peak abundance response in the mass
557 spectrometer. However, this assumption can bring some uncertainties because the ionization
558 efficiencies vary between different compounds (Schmidt et al., 2006; Leito et al., 2008; Perry et al.,
559 2008; Krueve et al., 2014). For example, the ionization efficiencies of nitrophenol species detected
560 in negative ESI mode can vary by a large degree depending on the position of the substituents at
561 the nitrobenzene ring (Schmidt et al., 2006; Krueve et al., 2014) and the ionization efficiencies of
562 carboxylic acids can also vary by several orders of magnitude depending on the structures (Krueve
563 et al., 2014). Nonetheless, it is a challenging analytical task to identify and quantify all compounds
564 in ambient OA due to the high chemical complexity of OA and the limits in authentic standards of
565 OA. Despite the inherent uncertainties, the peak abundance-weighted comparison of molecular
566 formulas provides an overview of the difference in chemical composition of OA in these three
567 representative Chinese cities. In particular, the chemical formulas assigned in this study can be
568 validated in future studies by authentic standards and the difference in ionization efficiencies can
569 be further evaluated.

570

571 **Author contributions.** RJH, TH and KW conducted the study design. LY, HN, JG and MW
572 collected the PM_{2.5} filter samples. KW and YZ carried out the experimental work and data analysis.

573 KW wrote the manuscript. KW, TH, RJH, M. Brüggemann, YZ, JH, M. Bilde and MG interpreted
574 data and edited the manuscript. All authors commented on and discussed the manuscript.

575 **Competing interests.** The authors declare that they have no conflict of interest.

576 **Acknowledgements.** This study was supported by the National Natural Science Foundation of
577 China (NSFC, Grant No. 41925015, No. 91644219 and No. 41877408), the Chinese Academy of
578 Sciences (No. ZDBS-LY-DQC001), the National Key Research and Development Program of
579 China (No. 2017YFC0212701), and the German Research Foundation (Deutsche
580 Forschungsgemeinschaft, DFG) under Grant No. INST 247/664-1 FUGG. K. Wang and Y. Zhang
581 acknowledge the scholarship from Chinese Scholarship Council (CSC) and Max Plank Graduate
582 Center with Johannes Gutenberg University of Mainz (MPGC) and thanks Prof. Ulrich Pöschl, Dr.
583 Christopher J. Kampf and Dr. Yafang Cheng for their helpful suggestion on this study. K. Wang
584 also thanks Dr. Huanfeng Dong from Zhejiang University for the great support on the programming
585 of data process.

586
587
588
589
590
591
592
593
594
595
596
597
598
599
600
601
602
603
604
605
606
607
608
609
610
611
612
613
614
615
616
617

618
619
620
621
622
623
624
625
626
627
628
629
630
631
632
633
634
635
636
637
638
639
640
641
642
643
644
645
646
647
648
649
650
651
652
653
654
655
656
657
658
659
660
661
662
663
664
665
666
667
668
669
670
671
672

References

- An, Z., Huang, R. J., Zhang, R., Tie, X., Li, G., Cao, J., Zhou, W., Shi, Z., Han, Y., Gu, Z., and Ji, Y.: Severe haze in northern China: A synergy of anthropogenic emissions and atmospheric processes, *Proc Natl Acad Sci U S A*, 116, 8657-8666, 10.1073/pnas.1900125116, 2019.
- Brüggemann, M., Poulain, L., Held, A., Stelzer, T., Zuth, C., Richters, S., Mutzel, A., van Pinxteren, D., Iinuma, Y., Katkevica, S., Rabe, R., Herrmann, H., and Hoffmann, T.: Real-time detection of highly oxidized organosulfates and BSOA marker compounds during the F-BEACH 2014 field study, *Atmos. Chem. Phys.*, 17, 1453-1469, 10.5194/acp-17-1453-2017, 2017.
- Brüggemann, M., van Pinxteren, D., Wang, Y., Yu, J. Z., and Herrmann, H.: Quantification of known and unknown terpenoid organosulfates in PM10 using untargeted LC-HRMS/MS: contrasting summertime rural Germany and the North China Plain, *Environmental Chemistry*, -, <https://doi.org/10.1071/EN19089>, 2019.
- Claeys, M., Graham, B., Vas, G., Wang, W., Vermeylen, R., Pashynska, V., Cafmeyer, J., Guyon, P., Andre, M., Artaxo, P., and Maenhaut, W.: Formation of secondary organic aerosol through photooxidation of isoprene, *Science*, 303, 1173-1175, 10.1126/science.1092805, 2004.
- Daellenbach, K. R., Kourtchev, I., Vogel, A. L., Bruns, E. A., Jiang, J., Petäjä, T., Jaffrezo, J.-L., Aksoyoglu, S., Kalberer, M., Baltensperger, U., El Haddad, I., and Prévôt, A. S. H.: Impact of anthropogenic and biogenic sources on the seasonal variation in the molecular composition of urban organic aerosols: a field and laboratory study using ultra-high-resolution mass spectrometry, *Atmospheric Chemistry and Physics*, 19, 5973-5991, 10.5194/acp-19-5973-2019, 2019.
- Ding, X., Zhang, Y.-Q., He, Q.-F., Yu, Q.-Q., Shen, R.-Q., Zhang, Y., Zhang, Z., Lyu, S.-J., Hu, Q.-H., Wang, Y.-S., Li, L.-F., Song, W., and Wang, X.-M.: Spatial and seasonal variations of secondary organic aerosol from terpenoids over China, *J. geophys. Res.-Atmos.*, 121, 14661-14678, doi:10.1002/2016JD025467, 2016.
- Elzein, A., Dunmore, R. E., Ward, M. W., Hamilton, J. F., and Lewis, A. C.: Variability of polycyclic aromatic hydrocarbons and their oxidative derivatives in wintertime Beijing, China, *Atmospheric Chemistry and Physics*, 19, 8741-8758, 10.5194/acp-19-8741-2019, 2019.
- Fleming, L. T., Lin, P., Laskin, A., Laskin, J., Weltman, R., Edwards, R. D., Arora, N. K., Yadav, A., Meinardi, S., Blake, D. R., Pillarisetti, A., Smith, K. R., and Nizkorodov, S. A.: Molecular composition of particulate matter emissions from dung and brushwood burning household cookstoves in Haryana, India, *Atmos. Chem. Phys.*, 18, 2461-2480, 10.5194/acp-18-2461-2018, 2018.
- Fu, P., Kawamura, K., Okuzawa, K., Aggarwal, S. G., Wang, G., Kanaya, Y., and Wang, Z.: Organic molecular compositions and temporal variations of summertime mountain aerosols over Mt. Tai, North China Plain, *J. Geophys. Res.*, 113, 10.1029/2008jd009900, 2008.
- Glasius, M., Hansen, A. M. K., Claeys, M., Henzing, J. S., Jedynska, A. D., Kasper-Giebl, A., Kistler, M., Kristensen, K., Martinsson, J., Maenhaut, W., Nøjgaard, J. K., Spindler, G., Stenström, K. E., Swietlicki, E., Szidat, S., Simpson, D., and Yttri, K. E.: Composition and sources of carbonaceous aerosols in Northern Europe during winter, *Atmos. Environ.*, 173, 127-141, 10.1016/j.atmosenv.2017.11.005, 2018.
- Hansen, A. M. K., Kristensen, K., Nguyen, Q. T., Zare, A., Cozzi, F., Noejgaard, J. K., Skov, H., Brandt, J., Christensen, J. H., Strom, J., Tunved, P., Krejci, R., and Glasius, M.: Organosulfates and organic acids in Arctic aerosols: speciation, annual variation and concentration levels, *Atmos. Chem. Phys.*, 14, 7807-7823, <https://doi.org/10.5194/acp-14-7807-2014>, 2014.
- Hansen, A. M. K., Hong, J., Raatikainen, T., Kristensen, K., Ylisirniö, A., Virtanen, A., Petäjä, T., Glasius, M., and Prisle, N. L.: Hygroscopic properties and cloud condensation nuclei activation of limonene-derived organosulfates and their mixtures with ammonium sulfate, *Atmos. Chem. Phys.*, 15, 14071-14089, <https://doi.org/10.5194/acp-15-14071-2015>, 2015.
- He, X., Huang, X. H. H., Chow, K. S., Wang, Q., Zhang, T., Wu, D., and Yu, J. Z.: Abundance and Sources of Phthalic Acids, Benzene-Tricarboxylic Acids, and Phenolic Acids in PM2.5 at Urban and Suburban

673 Sites in Southern China, *ACS Earth and Space Chemistry*, 2, 147-158,
674 10.1021/acsearthspacechem.7b00131, 2018.

675 Ho, C. S., Lam, C. W. K., Chan, M. H. M., Cheung, R. C. K., Law, L. K., Suen, M. W. M., and Tai, H. L.:
676 Electro spray ionisation mass spectrometry: principles and clinical application, *Clin. Biochem. Rev.*, 24,
677 10, 2003.

678 Hoffmann, T., Huang, R. J., and Kalberer, M.: Atmospheric analytical chemistry, *Anal. Chem.*, 83, 4649-
679 4664, 10.1021/ac2010718, 2011.

680 Huang, G., Liu, Y., Shao, M., Li, Y., Chen, Q., Zheng, Y., Wu, Z., Liu, Y., Wu, Y., Hu, M., Li, X., Lu, S.,
681 Wang, C., Liu, J., Zheng, M., and Zhu, T.: Potentially Important Contribution of Gas-Phase Oxidation of
682 Naphthalene and Methyl naphthalene to Secondary Organic Aerosol during Haze Events in Beijing,
683 *Environ Sci Technol*, 53, 1235-1244, 10.1021/acs.est.8b04523, 2019.

684 Huang, R. J., Zhang, Y., Bozzetti, C., Ho, K. F., Cao, J. J., Han, Y., Daellenbach, K. R., Slowik, J. G., Platt,
685 S. M., Canonaco, F., Zotter, P., Wolf, R., Pieber, S. M., Brun, E. A., Crippa, M., Ciarelli, G., Piazzalunga,
686 A., Schwikowski, M., Abbaszade, G., Schnelle-Kreis, J., Zimmermann, R., An, Z., Szidat, S.,
687 Baltensperger, U., El Haddad, I., and Prevot, A. S.: High secondary aerosol contribution to particulate
688 pollution during haze events in China, *Nature*, 514, 218-222, 10.1038/nature13774, 2014.

689 Huang, R. J., Cao, J. J., and Worsnop, D.: Sources and Chemical Composition of Particulate Matter During
690 Haze Pollution Events in China, in: *Air pollution in Eastern Asia: an integrated perspective*, edited by
691 Bouarar, I., Wang, X. M., and Brasseur, G. P., Springer, Cham, Switzerland, 49-68, 2017.

692 Iinuma, Y., Müller, C., Berndt, T., Böge, O., Claeys, M., and Herrmann, H.: Evidence for the existence of
693 organosulfates from β -pinene ozonolysis in ambient secondary organic aerosol, *Environ. Sci. Technol.*,
694 41, 6678-6683, 10.1021/es070938t, 2007.

695 Jung, J., and Kawamura, K.: Enhanced concentrations of citric acid in spring aerosols collected at the Gosan
696 background site in East Asia, *Atmos. Environ.*, 45, 5266-5272, 10.1016/j.atmosenv.2011.06.065, 2011.

697 Kautzman, K. E., Surratt, J. D., Chan, M. N., Chan, A. W., Hersey, S. P., Chhabra, P. S., Dalleska, N. F.,
698 Wennberg, P. O., Flagan, R. C., and Seinfeld, J. H.: Chemical composition of gas- and aerosol-phase
699 products from photooxidation of naphthalene, *J. Phys. Chem. A*, 114, 913-934, 10.1021/jp908530s, 2010.

700 Kind, T., and Fiehn, O.: Seven Golden Rules for heuristic filtering of molecular formulas obtained by
701 accurate mass spectrometry, *BMC Bioinformatics*, 8, 10.1186/1471-2105-8-105, 2007.

702 Kourtchev, I., O'Connor, I. P., Giorio, C., Fuller, S. J., Kristensen, K., Maenhaut, W., Wenger, J. C., Sodeau,
703 J. R., Glasius, M., and Kalberer, M.: Effects of anthropogenic emissions on the molecular composition of
704 urban organic aerosols: An ultrahigh resolution mass spectrometry study, *Atmo. Environ.*, 89, 525-532,
705 10.1016/j.atmosenv.2014.02.051, 2014.

706 Kourtchev, I., Godoi, R. H. M., Connors, S., Levine, J. G., Archibald, A. T., Godoi, A. F. L., Paralovo, S. L.,
707 Barbosa, C. G. G., Souza, R. A. F., Manzi, A. O., Seco, R., Sjostedt, S., Park, J.-H., Guenther, A., Kim,
708 S., Smith, J., Martin, S. T., and Kalberer, M.: Molecular composition of organic aerosols in central
709 Amazonia: an ultra-high-resolution mass spectrometry study, *Atmos. Chem. Phys.*, 16, 11899-11913,
710 <https://doi.org/10.5194/acp-16-11899-2016>, 2016.

711 Krueve, A., Kaupmees, K., Liigand, J., and Leito, I.: Negative electro spray ionization via deprotonation:
712 predicting the ionization efficiency, *Anal Chem*, 86, 4822-4830, 10.1021/ac404066v, 2014.

713 Laskin, A., Laskin, J., and Nizkorodov, S. A.: Chemistry of atmospheric brown carbon, *Chem. Rev.*, 115,
714 4335-4382, 10.1021/cr5006167, 2015.

715 Laskin, J., Laskin, A., Roach, P. J., Slysz, G. W., Anderson, G. A., Nizkorodov, S. A., Bones, D. L., and
716 Nguyen, L. Q.: High-Resolution Desorption Electro spray Ionization Mass Spectrometry for Chemical
717 Characterization of Organic Aerosols, *Anal. Chem.*, 82, 2048-2058, 10.1021/ac902801f, 2010.

718 Laskin, J., Laskin, A., and Nizkorodov, S. A.: Mass Spectrometry Analysis in Atmospheric Chemistry, *Anal.*
719 *Chem.*, 90, 166-189, 10.1021/acs.analchem.7b04249, 2018.

720 Lee, A., Goldstein, A. H., Kroll, J. H., Ng, N. L., Varutbangkul, V., Flagan, R. C., and Seinfeld, J. H.: Gas-
721 phase products and secondary aerosol yields from the photooxidation of 16 different terpenes, *J. Geophys.*
722 *Res.*, 111, 10.1029/2006jd007050, 2006.

723 Leito, I., Herodes, K., Huopola inen, M., Virro, K., Kunnas, A., Krueve, A., and Tanner, R.: Towards the
724 electro spray ionization mass spectrometry ionization efficiency scale of organic compounds, *Rapid*
725 *Commun Mass Spectrom*, 22, 379-384, 10.1002/rcm.3371, 2008.

726 Li, Y. J., Huang, D. D., Cheung, H. Y., Lee, A. K. Y., and Chan, C. K.: Aqueous-phase photochemical
727 oxidation and direct photolysis of vanillin – a model compound of methoxy phenols from biomass burning,

728 Atmospheric Chemistry and Physics, 14, 2871-2885, 10.5194/acp-14-2871-2014, 2014.
729 Lim, Y. B., Tan, Y., Perri, M. J., Seitzinger, S. P., and Turpin, B. J.: Aqueous chemistry and its role in
730 secondary organic aerosol (SOA) formation, *Atmos. Chem. Phys.*, 10, 10521-10539, 10.5194/acp-10-
731 10521-2010, 2010.
732 Lin, P., Rincon, A. G., Kalberer, M., and Yu, J. Z.: Elemental composition of HULIS in the Pearl River Delta
733 Region, China: results inferred from positive and negative electrospray high resolution mass
734 spectrometric data, *Environ. Sci. Technol.*, 46, 7454-7462, 10.1021/es300285d, 2012a.
735 Lin, P., Yu, J. Z., Engling, G., and Kalberer, M.: Organosulfates in humic-like substance fraction isolated
736 from aerosols at seven locations in East Asia: a study by ultra-high-resolution mass spectrometry, *Environ.*
737 *Sci. Technol.*, 46, 13118-13127, 10.1021/es303570v, 2012b.
738 Lin, P., Laskin, J., Nizkorodov, S. A., and Laskin, A.: Revealing Brown Carbon Chromophores Produced in
739 Reactions of Methylglyoxal with Ammonium Sulfate, *Environ. Sci. Technol.*, 49, 14257-14266,
740 10.1021/acs.est.5b03608, 2015.
741 McNeill, V. F., Woo, J. L., Kim, D. D., Schwier, A. N., Wannell, N. J., Sumner, A. J., and Barakat, J. M.:
742 Aqueous-phase secondary organic aerosol and organosulfate formation in atmospheric aerosols: a
743 modeling study, *Environ Sci Technol*, 46, 8075-8081, 10.1021/es3002986, 2012.
744 Ning, C., Gao, Y., Zhang, H., Yu, H., Wang, L., Geng, N., Cao, R., and Chen, J.: Molecular characterization
745 of dissolved organic matters in winter atmospheric fine particulate matters (PM_{2.5}) from a coastal city of
746 northeast China, *Sci Total Environ*, 689, 312-321, 10.1016/j.scitotenv.2019.06.418, 2019.
747 Nizkorodov, S. A., Laskin, J., and Laskin, A.: Molecular chemistry of organic aerosols through the
748 application of high resolution mass spectrometry, *Phys. Chem. Chem. Phys.*, 13, 3612-3629,
749 10.1039/c0cp02032j, 2011.
750 Noziere, B., Kalberer, M., Claeys, M., Allan, J., D'Anna, B., Decesari, S., Finessi, E., Glasius, M., Grgic, I.,
751 Hamilton, J. F., Hoffmann, T., Iinuma, Y., Jaoui, M., Kahnt, A., Kampf, C. J., Kourtschev, I., Maenhaut,
752 W., Marsden, N., Saarikoski, S., Schnelle-Kreis, J., Surratt, J. D., Szidat, S., Szmigielski, R., and
753 Wisthaler, A.: The molecular identification of organic compounds in the atmosphere: state of the art and
754 challenges, *Chem. Rev.*, 115, 3919-3983, 10.1021/cr5003485, 2015.
755 Pereira, K. L., Hamilton, J. F., Rickard, A. R., Bloss, W. J., Alam, M. S., Camredon, M., Muñoz, A., Vázquez,
756 M., Borrás, E., and Ródenas, M.: Secondary organic aerosol formation and composition from the photo-
757 oxidation of methyl chavicol (estragole), *Atmos. Chem. Phys.*, 14, 5349-5368, 10.5194/acp-14-5349-
758 2014, 2014.
759 Perry, R. H., Cooks, R. G., and Noll, R. J.: ORBITRAP MASS SPECTROMETRY: INSTRUMENTATION,
760 ION MOTION AND APPLICATIONS, *Mass Spectrometry Reviews*, 27, 661-699, 10.1002/mas.20186,
761 2008.
762 Rincón, A. G., Calvo, A. I., Dietzel, M., and Kalberer, M.: Seasonal differences of urban organic aerosol
763 composition - an ultra-high resolution mass spectrometry study, *Environ. Chem.*, 9, 298,
764 10.1071/en12016, 2012.
765 Riva, M., Tomaz, S., Cui, T., Lin, Y.-H., Perraudin, E., Gold, A., Stone, E. A., Villenave, E., and Surratt, J.
766 D.: Evidence for an Unrecognized Secondary Anthropogenic Source of Organosulfates and Sulfonates:
767 Gas-Phase Oxidation of Polycyclic Aromatic Hydrocarbons in the Presence of Sulfate Aerosol, *Environ.*
768 *Sci. Technol.*, 49, 6654-6664, 10.1021/acs.est.5b00836, 2015.
769 Schmidt, A. C., Herzsuh, R., Matsysik, F. M., and Engewald, W.: Investigation of the ionisation and
770 fragmentation behaviour of different nitroaromatic compounds occurring as polar metabolites of
771 explosives using electrospray ionisation tandem mass spectrometry, *Rapid Commun Mass Spectrom*, 20,
772 2293-2302, 10.1002/rcm.2591, 2006.
773 Shi, Z., Vu, T., Kotthaus, S., Harrison, R. M., Grimmond, S., Yue, S., Zhu, T., Lee, J., Han, Y., Demuzere,
774 M., Dunmore, R. E., Ren, L., Liu, D., Wang, Y., Wild, O., Allan, J., Acton, W. J., Barlow, J., Barratt, B.,
775 Beddows, D., Bloss, W. J., Calzolari, G., Carruthers, D., Carslaw, D. C., Chan, Q., Chatzidiakou, L., Chen,
776 Y., Crilley, L., Coe, H., Dai, T., Doherty, R., Duan, F., Fu, P., Ge, B., Ge, M., Guan, D., Hamilton, J. F.,
777 He, K., Heal, M., Heard, D., Hewitt, C. N., Hollaway, M., Hu, M., Ji, D., Jiang, X., Jones, R., Kalberer,
778 M., Kelly, F. J., Kramer, L., Langford, B., Lin, C., Lewis, A. C., Li, J., Li, W., Liu, H., Liu, J., Loh, M.,
779 Lu, K., Lucarelli, F., Mann, G., McFiggans, G., Miller, M. R., Mills, G., Monk, P., Nemitz, E., amp, apos,
780 Connor, F., Ouyang, B., Palmer, P. I., Percival, C., Popoola, O., Reeves, C., Rickard, A. R., Shao, L., Shi,
781 G., Spracklen, D., Stevenson, D., Sun, Y., Sun, Z., Tao, S., Tong, S., Wang, Q., Wang, W., Wang, X.,
782 Wang, X., Wang, Z., Wei, L., Whalley, L., Wu, X., Wu, Z., Xie, P., Yang, F., Zhang, Q., Zhang, Y.,

783 Zhang, Y., and Zheng, M.: Introduction to the special issue “In-depth study of air pollution sources and
784 processes within Beijing and its surrounding region (APHH-Beijing)”, *Atmospheric Chemistry and*
785 *Physics*, 19, 7519-7546, 10.5194/acp-19-7519-2019, 2019.

786 Song, J., Li, M., Jiang, B., Wei, S., Fan, X., and Peng, P.: Molecular Characterization of Water-Soluble
787 Humic like Substances in Smoke Particles Emitted from Combustion of Biomass Materials and Coal
788 Using Ultrahigh-Resolution Electrospray Ionization Fourier Transform Ion Cyclotron Resonance Mass
789 Spectrometry, *Environ. Sci. Technol.*, 52, 2575-2585, 10.1021/acs.est.7b06126, 2018.

790 Sun, Y., Jiang, Q., Zhang, Z., Fu, P., Li, J., Yang, T., and Yin, Y.: Investigation of the sources and evolution
791 processes of severe haze pollution in Beijing in January 2013, *J. Geophys. Res.-Atmos.*, 119, 4380-4389,
792 10.1002/, 2014.

793 Surratt, J. D., Gomez-Gonzalez, Y., Chan, A. W., Vermeylen, R., Shahgholl, M., Kleindienst, T. E., Jaoui,
794 M., Maenhaut, W., Claeys, M., Flagan, R. C., and Seinfeld, J. H.: Evidence for Organosulfate in
795 Secondary Organic Aerosol, *Environ. Sci. Technol.*, 41, 517-527, 10.1021/es062081q, 2007.

796 Surratt, J. D., Gómez-González, Y., Chan, A. W., Vermeylen, R., Shahgholi, M., Kleindienst, T. E., Edney,
797 E. O., Offenberg, J. H., Lewandowski, M., Jaoui, M., Maenhaut, W., Claeys, M., Flagan, R. C., and
798 Seinfeld, J. H.: Organosulfate Formation in Biogenic Secondary Organic Aerosol, *J. Phys. Chem. A*, 112,
799 8345-8378, 2008.

800 Tao, S., Lu, X., Levac, N., Bateman, A. P., Nguyen, T. B., Bones, D. L., Nizkorodov, S. A., Laskin, J., Laskin,
801 A., and Yang, X.: Molecular Characterization of Organosulfates in Organic Aerosols from Shanghai and
802 Los Angeles Urban Areas by Nanospray-Desorption Electrospray Ionization High-Resolution Mass
803 Spectrometry, *Environ. Sci. Technol.*, 48, 10993-11001, 10.1021/es5024674, 2014.

804 Tong, H., Kourtchev, I., Pant, P., Keyte, I. J., O'Connor, I. P., Wenger, J. C., Pope, F. D., Harrison, R. M.,
805 and Kalberer, M.: Molecular composition of organic aerosols at urban background and road tunnel sites
806 using ultra-high resolution mass spectrometry, *Faraday Discuss.*, 189, 51-68, 10.1039/c5fd00206k, 2016.

807 Tong, H., Zhang, Y., Filippi, A., Wang, T., Li, C., Liu, F., Leppla, D., Kourtchev, I., Wang, K., Keskinen, H.
808 M., Levula, J. T., Arangio, A. M., Shen, F., Ditas, F., Martin, S. T., Artaxo, P., Godoi, R. H. M.,
809 Yamamoto, C. I., de Souza, R. A. F., Huang, R. J., Berkemeier, T., Wang, Y., Su, H., Cheng, Y., Pope,
810 F. D., Fu, P., Yao, M., Pohlker, C., Petaja, T., Kulmala, M., Andreae, M. O., Shiraiwa, M., Poschl, U.,
811 Hoffmann, T., and Kalberer, M.: Radical Formation by Fine Particulate Matter Associated with Highly
812 Oxygenated Molecules, *Environ Sci Technol*, 53, 12506-12518, 10.1021/acs.est.9b05149, 2019.

813 Tu, P., Hall, W. A. t., and Johnston, M. V.: Characterization of Highly Oxidized Molecules in Fresh and
814 Aged Biogenic Secondary Organic Aerosol, *Anal. Chem.*, 88, 4495-4501,
815 10.1021/acs.analchem.6b00378, 2016.

816 Wang, G., Kawamura, K., Umemoto, N., Xie, M., Hu, S., and Wang, Z.: Water-soluble organic compounds
817 in PM_{2.5} and size-segregated aerosols over Mount Tai in North China Plain, *J. Geophys. Res.*, 114,
818 10.1029/2008jd011390, 2009.

819 Wang, K., Zhang, Y., Huang, R.-J., Cao, J., and Hoffmann, T.: UHPLC-Orbitrap mass spectrometric
820 characterization of organic aerosol from a central European city (Mainz, Germany) and a Chinese
821 megacity (Beijing), *Atmos. Environ.*, 189, 22-29, 10.1016/j.atmosenv.2018.06.036, 2018.

822 Wang, K., Zhang, Y., Huang, R.-J., Wang, M., Ni, H., Kampf, C. J., Cheng, Y., Bilde, M., Glasius, M., and
823 Hoffmann, T.: Molecular characterization and source identification of atmospheric particulate
824 organosulfates using ultrahigh resolution mass spectrometry, *Environ. Sci. Technol.*,
825 10.1021/acs.est.9b02628, 2019a.

826 Wang, M., Huang, R.-J., Cao, J., Dai, W., Zhou, J., Lin, C., Ni, H., Duan, J., Wang, T., Chen, Y., Li, Y.,
827 Chen, Q., Haddad, I. E., and Hoffmann, T.: Determination of n-alkanes, PAHs and hopanes in
828 atmospheric aerosol: evaluation and comparison of thermal desorption GC-MS and solvent extraction
829 GC-MS approaches, *Atmos. Mea. Tech. Discuss.*, 1-21, 10.5194/amt-2019-4, 2019b.

830 Wang, X. K., Rossignol, S., Ma, Y., Yao, L., Wang, M. Y., Chen, J. M., George, C., and Wang, L.: Molecular
831 characterization of atmospheric particulate organosulfates in three megacities at the middle and lower
832 reaches of the Yangtze River, *Atmos. Chem. Phys.*, 16, 2285-2298, [https://doi.org/10.5194/acp-16-2285-](https://doi.org/10.5194/acp-16-2285-2016)
833 [2016](https://doi.org/10.5194/acp-16-2285-2016), 2016.

834 Wang, X. K., Hayeck, N., Brüggemann, M., Yao, L., Chen, H. F., Zhang, C., Emmelin, C., Chen, J. M.,
835 George, C., and Wang, L.: Chemical characterization of organic aerosol in: A study by Ultrahigh-
836 Performance Liquid Chromatography Coupled with Orbitrap Mass Spectrometry, *J. Geophys. Res.-Atmos.*,
837 122, 703-722, <https://doi.org/10.1002/2017JD026930>, 2017.

838 Xu, W., Sun, Y., Wang, Q., Zhao, J., Wang, J., Ge, X., Xie, C., Zhou, W., Du, W., Li, J., Fu, P., Wang, Z.,
839 Worsnop, D. R., and Coe, H.: Changes in Aerosol Chemistry From 2014 to 2016 in Winter in Beijing:
840 Insights From High-Resolution Aerosol Mass Spectrometry, *J. Geophys. Res.-Atmos.*, 124, 1132-1147,
841 10.1029/2018jd029245, 2019.

842 Yassine, M. M., Harir, M., Dabek-Zlotorzynska, E., and Schmitt-Kopplin, P.: Structural characterization of
843 organic aerosol using Fourier transform ion cyclotron resonance mass spectrometry: aromaticity
844 equivalent approach, *Rapid Commun. Mass Spectrom.*, 28, 2445-2454, 10.1002/rcm.7038, 2014.

845 Zhang, P.: Revitalizing old industrial base of Northeast China: Process, policy and challenge, *Chin. Geogra.*
846 *Sci.*, 18, 109-118, 10.1007/s11769-008-0109-2, 2008.

847 Zielinski, A. T., Kourtchev, I., Bortolini, C., Fuller, S. J., Giorio, C., Popoola, O. A. M., Bogialli, S., Tapparo,
848 A., Jones, R. L., and Kalberer, M.: A new processing scheme for ultra-high resolution direct infusion
849 mass spectrometry data, *Atmos. Environ.*, 178, 129-139, 10.1016/j.atmosenv.2018.01.034, 2018.

850

851

852

853

854

855

856

857

858

859

860

861

862

863

864

865

866

867

868

869

870

871

872

873

874

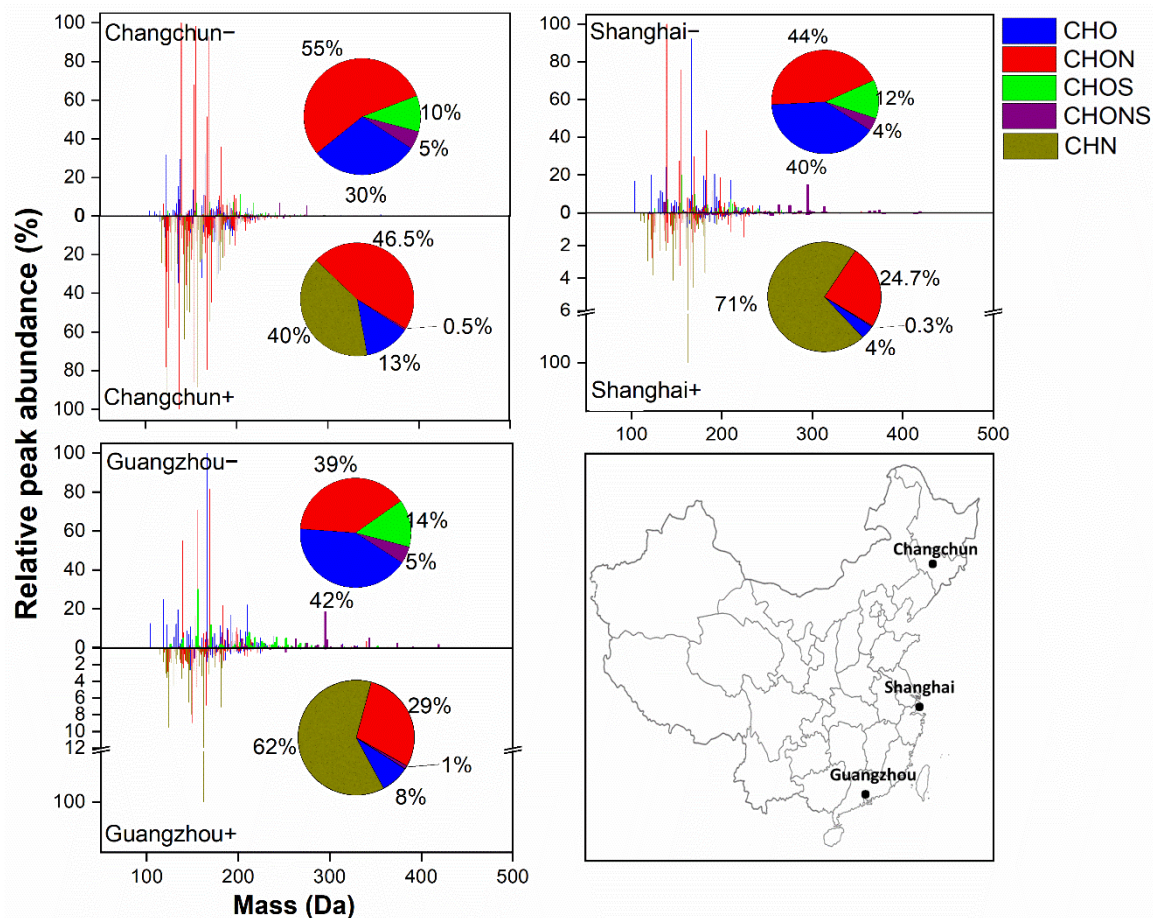
875

876 Table 1. Number of organic compounds and molecular formulas in each subgroup and the peak
 877 abundance-weighted average values of molecular mass (MM_{avg}), elemental ratios, double bond
 878 equivalent (DBE), aromaticity equivalent (X_c) and isomer number fraction (meaning the
 879 percentage of formula numbers that have isomers among all assigned formulas) for detected
 880 organic compounds in ESI⁻ and ESI⁺ in the three Chinese cities.

Sample ID	Subgroup	Number of compounds*	Relative abundance (%)	MM_{avg}	H/C	O/C**	DBE	X_c	Isomer number fraction (%)
Changchun ⁻	total	769(415)	100	169	1.03	0.58	5.02	2.13	34
	CHO ⁻	346(136)	30	162	0.96	0.41	5.65	2.28	52
	CHON ⁻	180(96)	55	163	0.94	0.51	5.24	2.44	36
	CHOS ⁻	155(105)	10	198	1.56	1.17(0.52)	2.55	0.50	28
	CHONS ⁻	88(78)	5	214	1.35	1.07(-1.4)	3.75	1.06	8
Shanghai ⁻	total	416(272)	100	176	1.05	0.69	4.99	1.92	31
	CHO ⁻	164(90)	40	171	0.97	0.59	5.37	1.94	41
	CHON ⁻	135(89)	44	169	0.86	0.56	5.67	2.47	37
	CHOS ⁻	75(62)	12	190	1.85	1.41(0.61)	1.79	0.34	15
	CHONS ⁻	42(31)	4	266	1.56	1.00(0.11)	3.30	0.44	13
Guangzhou ⁻	total	488(304)	100	183	1.14	0.74	4.55	1.65	34
	CHO ⁻	196(110)	42	172	1.10	0.65	4.68	1.57	44
	CHON ⁻	161(98)	39	173	0.89	0.58	5.56	2.41	35
	CHOS ⁻	86(67)	14	201	1.85	1.48(0.71)	1.71	0.21	21
	CHONS ⁻	45(29)	5	293	1.56	0.82(0.06)	3.45	0.43	28
Changchun ⁺	total	2943(679)	100	160	1.21	0.13	5.58	2.36	56
	CHO ⁺	609(162)	13	174	0.94	0.28	6.55	2.22	50
	CHN ⁺	696(126)	40	154	1.22	0.00	5.84	2.60	77
	CHON ⁺	1594(352)	46.5	161	1.27	0.19	5.11	2.22	55
	CHONS ⁺	44(39)	0.5	196	1.91	0.70	2.64	0.09	13
Shanghai ⁺	total	704(383)	100	162	1.37	0.09	4.91	2.32	32
	CHO ⁺	87(67)	4	184	1.13	0.43	5.46	1.46	19
	CHN ⁺	253(84)	71	159	1.38	0.00	5.08	2.55	54
	CHON ⁺	350(218)	24.7	167	1.40	0.27	4.34	1.81	30
	CHONS ⁺	14(14)	0.3	241	1.17	0.61	5.32	0.91	0
Guangzhou ⁺	total	687(412)	100	161	1.41	0.17	4.58	2.07	30
	CHO ⁺	125(87)	8	185	1.12	0.42	5.19	1.20	26
	CHN ⁺	205(78)	62	156	1.42	0.00	4.80	2.47	54
	CHON ⁺	336(227)	29	165	1.47	0.45	4.00	1.51	26

881 *The values in brackets indicate the number of unique molecular formulas. **The values in brackets indicate the
 882 (O-3S)/C and (O-3S-2N)/C ratios for CHOS and CHONS compounds, respectively, detected in ESI- mode

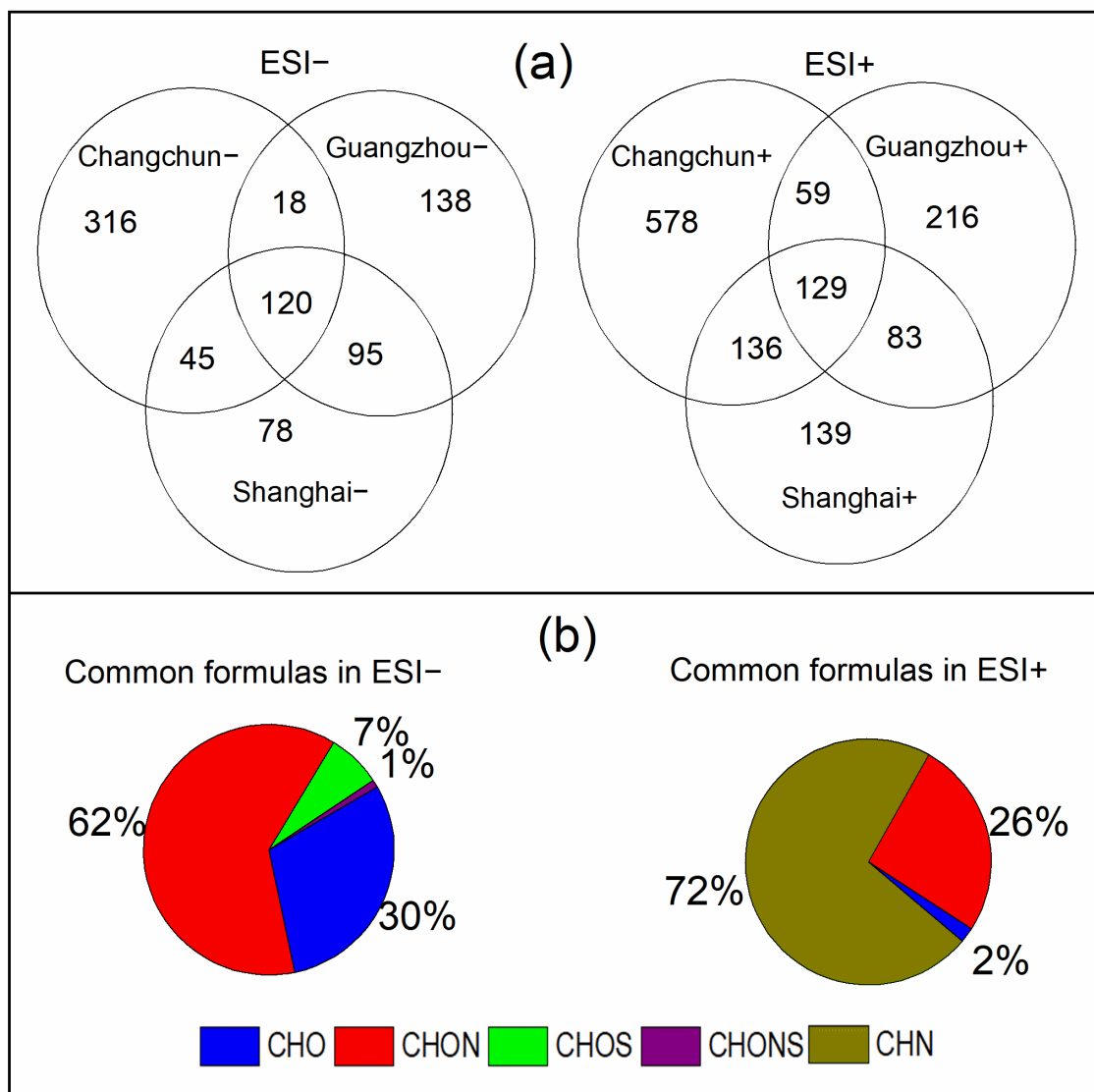
883



884

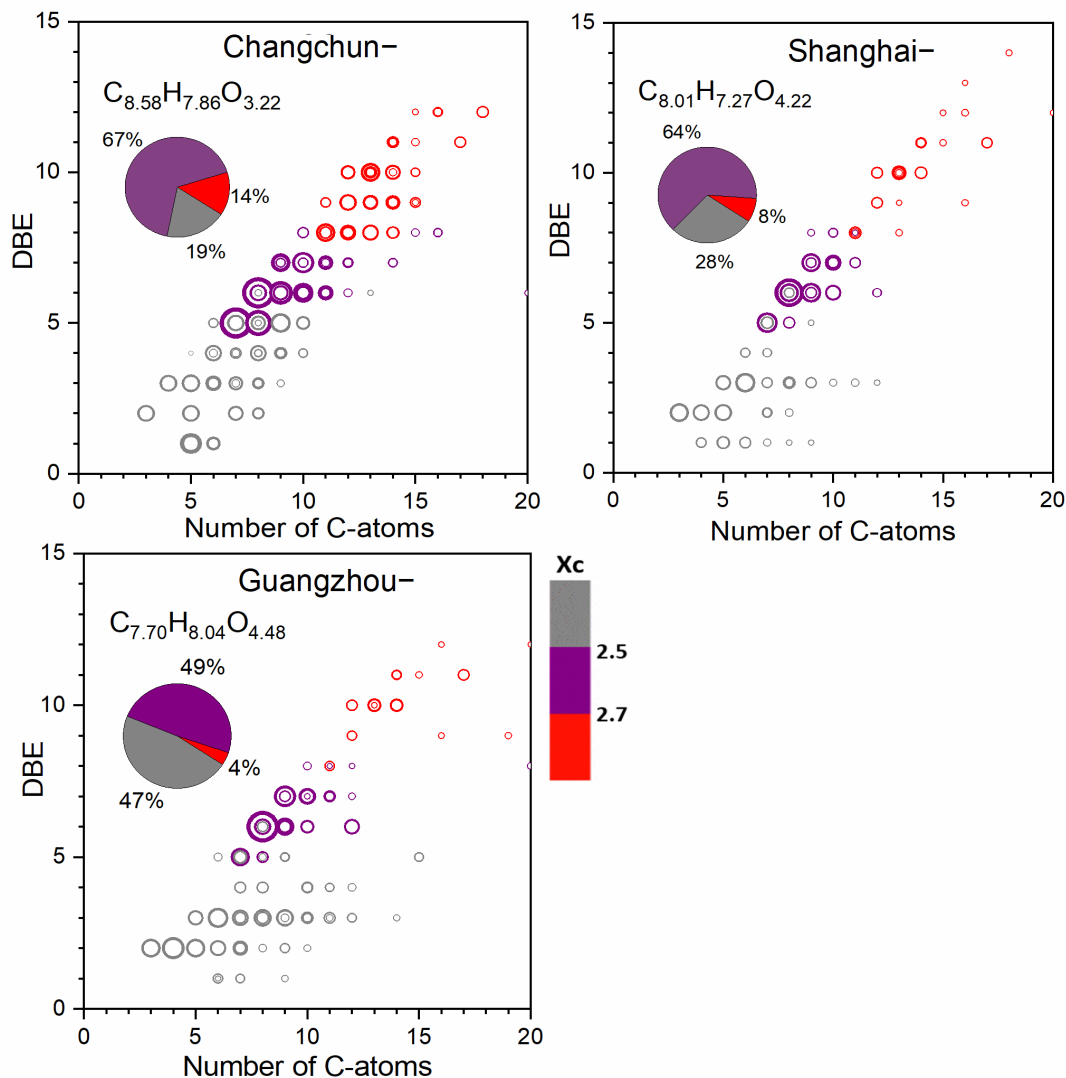
885 Figure 1. Mass spectra of detected organic compounds reconstructed from extracted ion
 886 chromatograms in ESI- and ESI+. The horizontal axis refers to the molecular mass (Da) of the
 887 identified species. The vertical axis refers to the relative peak abundance of each individual
 888 compound to the compound with the greatest peak abundance. The pie charts show the percentage
 889 of each organic compound subgroup (i.e. CHO, CHON, CHOS, CHONS and CHN) in each sample
 890 in terms of peak abundance. The map in the lower right corner shows the locations of these three
 891 megacities in China.

892



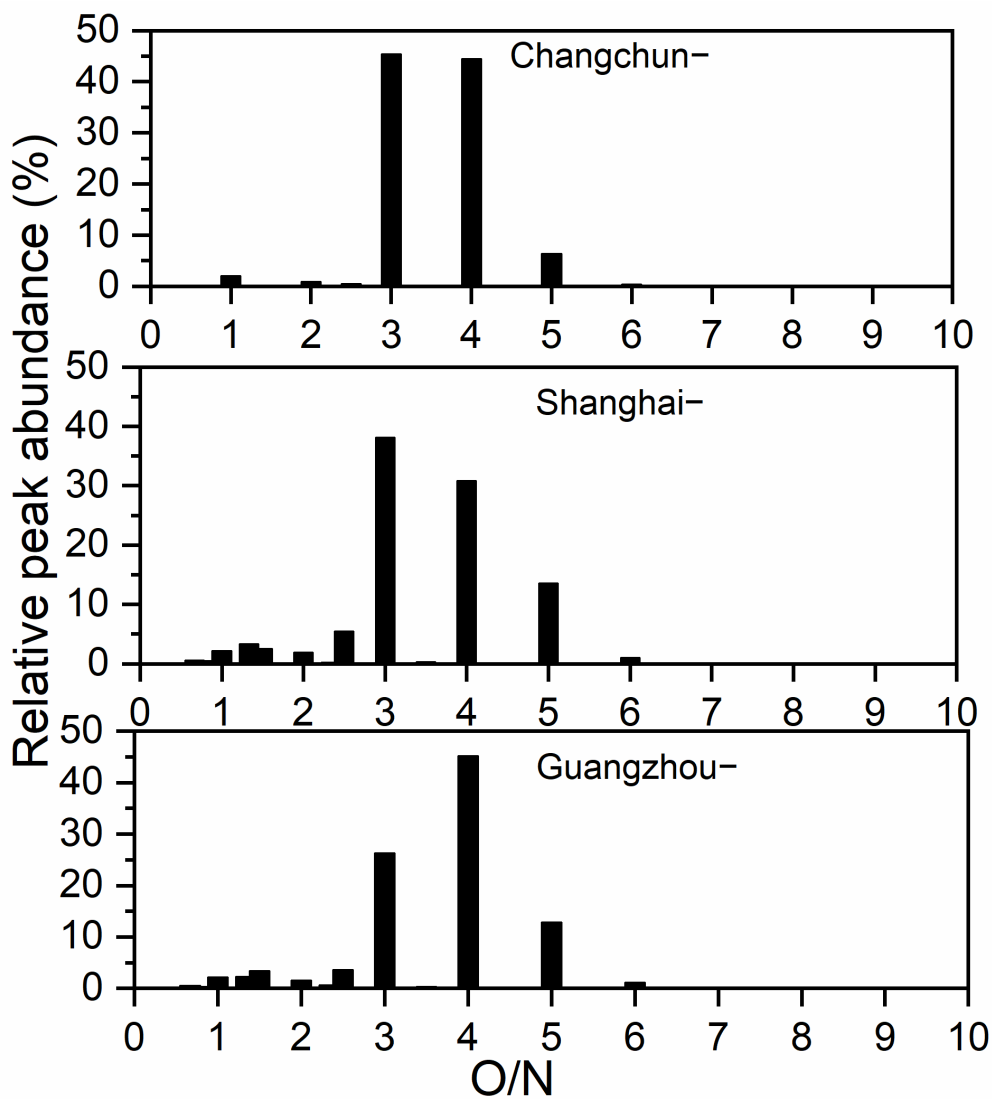
893

894 Figure 2. (a) Venn diagrams showing the number distribution of all molecular formulas detected in
 895 ESI- and ESI+ for all sample locations. The overlapping molecular formulas refer to the
 896 compounds detected in each city with the same molecular formulas and with the same retention
 897 times (retention time difference ≤ 0.1 min). (b) Peak abundance contribution of each elemental
 898 formula category to the total common formulas.



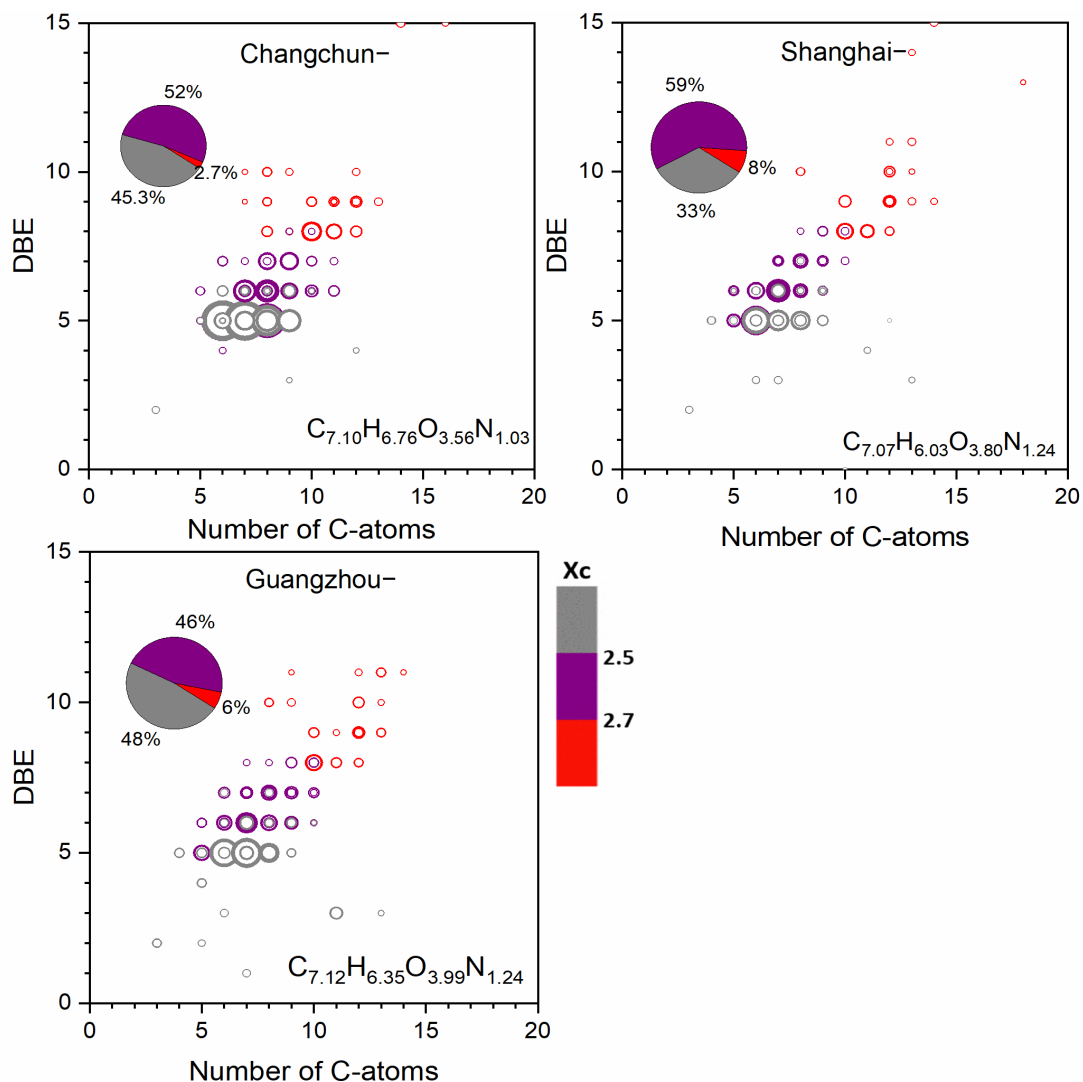
899

900 Figure 3. Double bond equivalent (DBE) versus carbon number for all CHO- compounds for all
 901 sample locations. The molecular formula represents the abundance-weighted average CHO-
 902 formula and the area of the circles is proportional to the fourth root of the peak abundance of an
 903 individual compound (a diagram with circle areas related to the absolute peak abundances is
 904 presented in Fig. S2). The color bar denotes the aromaticity equivalent (gray with $X_c < 2.50$, purple
 905 with $2.50 \leq X_c < 2.70$ and red with $X_c \geq 2.70$). The pie charts show the percentage of each X_c
 906 category (i.e., gray color-coded compounds, purple color-coded compounds and red color-coded
 907 compounds) in each sample in terms of peak abundance.



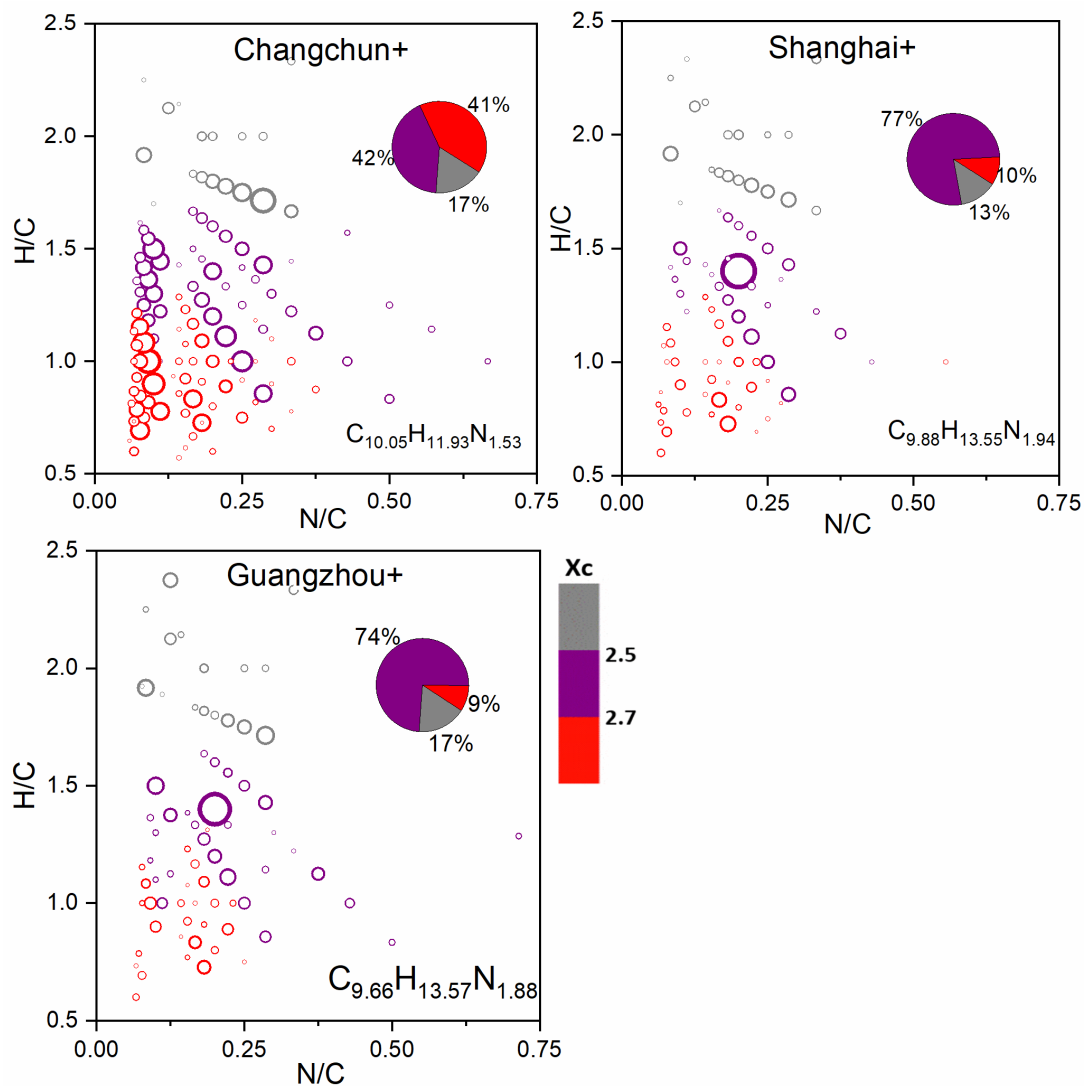
908

909 Figure 4. Classification of CHON⁻ compounds into different subgroups according to O/N ratios in
 910 their formulas. The y-axis indicates the relative contribution of each specific O/N ratio subgroup to
 911 the sum of peak abundances of CHON⁻ compounds.



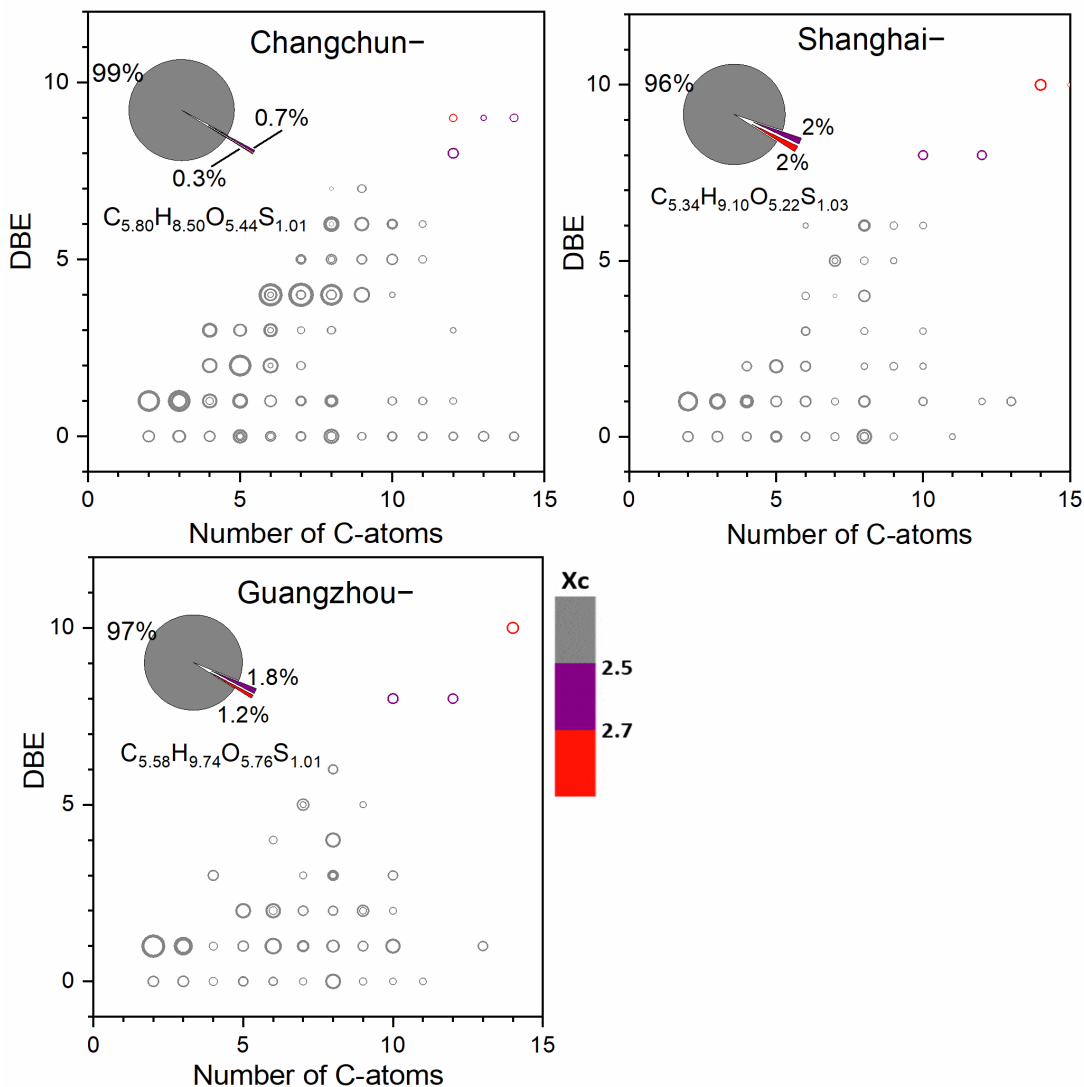
912

913 Figure 5. Double bond equivalent (DBE) versus carbon number for all CHON-
 914 sample locations. The molecular formula represents the abundance-weighted average CHON-
 915 formula and the area of circles is proportional to the fourth root of the peak abundance of an
 916 individual compound (a diagram with circle areas related to absolute peak abundances is presented
 917 in Fig. S6). The color bar denotes the aromaticity equivalent (gray with $X_c < 2.50$, purple with 2.50
 918 $\leq X_c < 2.70$ and red with $X_c \geq 2.70$). The pie charts show the percentage of each X_c category (i.e.,
 919 gray color-coded compounds, purple color-coded compounds and red color-coded compounds) in
 920 each sample in terms of peak abundance.



921

922 Figure 6. Van Krevelen diagrams for CHN+ compounds in Changchun, Shanghai and Guangzhou
 923 samples. The area of circles is proportional to the fourth root of the peak abundance of an individual
 924 compound (a diagram with circle areas related to absolute peak abundances is presented in Fig.
 925 S10) and the color bar denotes the aromaticity equivalent (gray with $X_c < 2.50$, purple with $2.50 \leq$
 926 $X_c < 2.70$ and red with $X_c \geq 2.70$). The pie charts show the percentage of each X_c category (i.e.,
 927 gray color-coded compounds, purple color-coded compounds and red color-coded compounds) in
 928 each sample in terms of peak abundance.



929

930 Figure 7. Double bond equivalent (DBE) versus carbon number for all CHOS-
 931 compounds for all sample locations. The molecular formula represents the abundance-weighted average CHOS-
 932 formula and the area of circles is proportional to the fourth root of the peak abundance of an
 933 individual compound (a diagram with circle areas related to absolute peak abundances is presented
 934 in Fig. S11). The color bar denotes the aromaticity equivalent (gray with $X_c < 2.50$, purple with
 935 $2.50 \leq X_c < 2.70$ and red with $X_c \geq 2.70$). The pie charts show the percentage of each X_c category
 936 (i.e., gray color-coded compounds, purple color-coded compounds and red color-coded compounds)
 937 in each sample in terms of peak abundance.

938

939

940